



**YACHAY UNIVERSITY OF EXPERIMENTAL
TECHNOLOGY AND RESEARCH**

SCHOOL OF CHEMICAL SCIENCE AND ENGINEERING

**TITLE: EVALUATION OF THE REDUCING AND
CAPPING AGENT OF GARLIC AND CINNAMON BARK
EXTRACTS IN THE SYNTHESIS OF SILVER
NANOPARTICLES**

Curriculum integration work presented as a requirement to
obtain the Chemistry degree

Author:

Granja Alvear Lourdes Araceli
araceligranja86@gmail.com

Advisor:

PhD. López González Floralba
flopez@yachaytech.edu.ec

Urcuquí, August 2019

Urcuquí, 19 de agosto de 2019

SECRETARÍA GENERAL
(Vicerrectorado Académico/Cancillería)
ESCUELA DE CIENCIAS QUÍMICAS E INGENIERÍA
CARRERA DE QUÍMICA
ACTA DE DEFENSA No. UITEY-CHE-2019-00001-AD

En la ciudad de San Miguel de Urcuquí, Provincia de Imbabura, a los 19 días del mes de agosto de 2019, a las 15:00 horas, en el Aula AI-101 de la Universidad de Investigación de Tecnología Experimental Yachay y ante el Tribunal Calificador, integrado por los docentes:

<u>Presidente Tribunal de Defensa</u>	<u>VILORIA VERA, DARIO ALFREDO</u>
<u>Miembro No Tutor</u>	<u>BRICEÑO ARAUJO, SARAH ELISA</u>
<u>Tutor</u>	<u>LOPEZ GONZALEZ, FLORALBA AGGENY</u>

Se presenta el(la) señor(ita) estudiante **GRANJA ALVEAR, LOURDES ARACELI**, con cédula de identidad No. **1003444039**, de la **ESCUELA DE CIENCIAS QUÍMICAS E INGENIERÍA**, de la Carrera de **QUÍMICA**, aprobada por el Consejo de Educación Superior (CES), mediante Resolución **RPC-SO-39-No.456-2014**, con el objeto de rendir la sustentación de su trabajo de titulación denominado: **Evaluation of the Reducing and Capping Agent of Garlic and Cinnamon Bark extracts in the Synthesis of Silver Nanoparticles**, previa a la obtención del título de **QUÍMICO/A**.

El citado trabajo de titulación, fue debidamente aprobado por el(los) docente(s):

Tutor LOPEZ GONZALEZ, FLORALBA AGGENY


Y recibió las observaciones de los otros miembros del Tribunal Calificador, las mismas que han sido incorporadas por el(la) estudiante.

Previamente cumplidos los requisitos legales y reglamentarios, el trabajo de titulación fue sustentado por el(la) estudiante y examinado por los miembros del Tribunal Calificador. Escuchada la sustentación del trabajo de titulación, que integró la exposición de el(la) estudiante sobre el contenido de la misma y las preguntas formuladas por los miembros del Tribunal, se califica la sustentación del trabajo de titulación con las siguientes calificaciones:

Tipo	Docente	Calificación
Tutor	LOPEZ GONZALEZ, FLORALBA AGGENY	9,9
Presidente Tribunal De Defensa	VILORIA VERA, DARIO ALFREDO	10,0
Miembro Tribunal De Defensa	BRICEÑO ARAUJO, SARAH ELISA	9,6

Lo que da un promedio de: **9.8 (Nueve punto Ocho)**, sobre 10 (diez), equivalente a: **APROBADO**

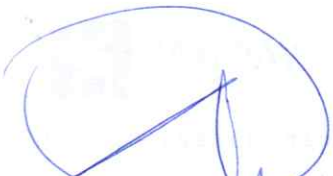
Para constancia de lo actuado, firman los miembros del Tribunal Calificador, el/la estudiante y el/la secretario ad-hoc.


GRANJA ALVEAR, LOURDES ARACELI
Estudiante


VILORIA VERA, DARIO ALFREDO
Presidente Tribunal de Defensa


LOPEZ GONZALEZ, FLORALBA AGGENY
Tutor





BRICEÑO ARAUJO, SARAFELISA
~~Miembro No Tutor~~

[Handwritten Signature]

ESCOBAR LANDAZURI, ANA MARIA
Secretario Ad-hoc

SECRETARÍA GENERAL
[Instituto de Asesoría Científica]
ESCUELA DE CIENCIAS QUÍMICAS E INGENIERÍA
CARRERA DE QUÍMICA
ACTA DE DEFENSA No. UTBY-CH-2019-0001-AD

Tutor: _____
Miembro No-Tutor: _____
Presidente Tribunal de Defensa: _____

Se presenta el Tesis de grado de GRADUATE IN CHEMISTRY, JORDAN ALFREDO, con tema de tesis: "Sintesis de un compuesto organico a partir de reactivos de laboratorio".
El Tesis de grado de GRADUATE IN CHEMISTRY, JORDAN ALFREDO, con tema de tesis: "Sintesis de un compuesto organico a partir de reactivos de laboratorio".

El Tesis de grado de GRADUATE IN CHEMISTRY, JORDAN ALFREDO, con tema de tesis: "Sintesis de un compuesto organico a partir de reactivos de laboratorio".
El Tesis de grado de GRADUATE IN CHEMISTRY, JORDAN ALFREDO, con tema de tesis: "Sintesis de un compuesto organico a partir de reactivos de laboratorio".

Nombre	Apellido	Identificación
JORDAN ALFREDO	ALFREDO	101010101010101010
ALFREDO ALFREDO	ALFREDO	101010101010101010
ALFREDO ALFREDO	ALFREDO	101010101010101010

[Handwritten Signature]
ALFREDO ALFREDO ALFREDO
SECRETARÍA GENERAL
[Instituto de Asesoría Científica]

AUTORÍA

Yo, **Lourdes Araceli Granja Alvear**, con cédula de identidad 1003444039, declaro que las ideas, juicios, valoraciones, interpretaciones, consultas bibliográficas, definiciones y conceptualizaciones expuestas en el presente trabajo; así cómo, los procedimientos y herramientas utilizadas en la investigación, son de absoluta responsabilidad de la autora del trabajo de integración curricular. Así mismo, me acojo a los reglamentos internos de la Universidad de Investigación de Tecnología Experimental Yachay.

Urcuquí, Agosto 2019.



Lourdes Araceli Granja Alvear

CI: 1003444039

AUTORIZACIÓN DE PUBLICACIÓN

Yo **Lourdes Araceli Granja Alvear**, con cédula de identidad 1003444039 cedo a la Universidad de Tecnología Experimental Yachay, los derechos de publicación de la presente obra, sin que deba haber un reconocimiento económico por este concepto. Declaro además que el texto del presente trabajo de titulación no podrá ser cedido a ninguna empresa editorial para su publicación u otros fines, sin contar previamente con la autorización escrita de la Universidad

Asimismo, autorizo a la Universidad que realice la digitalización y publicación de este trabajo de integración curricular en el repositorio virtual, de conformidad a lo dispuesto en el Art. 144 de la Ley Orgánica de Educación Superior

Urcuquí, Agosto 2019



Lourdes Araceli Granja Alvear

CI: 1003444039

Acknowledgments

I want to thank all the people who made it possible for this work to be successfully developed. Firstly, my advisor Floralba Lopez PhD, and my co-author Juan Pablo Saucedo PhD., a special thanks to Hortensia Rodriguez, Dean of the School of Chemical Sciences and Engineering for all the facilities she has given me to carry out all the activities that were required to perform the projected a special thanks to Yachay Tech University.

I also thank Jose Angel Rivera, Thibault Terencio, Juan Pablo Tafur, Gottfried Suppan and Alex Palma Professors of the School and Professor Gema González of School of Physics for being an essential part in this stage of my academic training.

A special thanks to Nayely Pineda PhD, member of CIMAV-Monterrey, Also to Patricia Lozano PhD, and Elena Bello M.C., from the University of Puebla BUAP, Ivan Peña M.C ICUAP Puebla for allowing me to do part of my graduated project in their laboratories.

Dedication

I dedicate this work to my little daughter **Danna Aguirre**, since She has been my inspiration since the first day I entered the University, with the motivation of forming me to be a good professional and an example for her. Especially because many hours together were sacrificed to fulfill my obligations as a student.

This stage of my academic life is also dedicated to each member of my family, because thanks to them I have been able to reach the challenges that were presented to me. Thanks to the support he always gave me; Victor, my life partner. To my Mother and my sisters Lorena and Diana who always gave me their support and unconditional love.

ABSTRACT:

A procedure for the synthesis of silver nanoparticles is presented in which their size is controlled modulating nucleation and particle growth processes by means of suitable proportions of reducing and capping agents. Colloidal dispersions of nanoparticles were obtained, which were evidenced by the Surface Plasmon Resonance exhibited in a wavelength range of the radio-magnetic spectrum from 400 nm to 700 nm, corresponding from spherical nanoparticles to nanoprisms. In addition, we show the effectiveness of garlic extract, whose main component is Allicin, and the cinnamon bark extract, whose main component is the Cinnamaldehyde, as reducing and capping agents in the process of nanoparticle synthesis. The stability of the colloidal dispersion extends for several weeks. Some conductivity of silver nanoparticles embedded in pectin films was also evidenced. In addition antibacterial effect was analyzed. The presence of silver nanoparticles with different shapes was evidenced by the signal of Surface Plasmon Resonance detected by UV Spectroscopy, which were corroborated by Scanning Transmission Electron Microscopy (STEM) and Dynamic Light Scattering (DLS), using the Z potential to determine the size of the nanoparticles obtained with these syntheses, besides the morphology of them.

KEYWORDS:

Silver Nanoparticles, morphology nanostructure, Surface Plasmon Resonance (SPR) garlic extract, cinnamon bark extract, allicin, cinnamaldehyde.

RESUMEN:

Se presenta un procedimiento para la síntesis de nanopartículas de plata en el que se controla su tamaño modulando los procesos de nucleación y crecimiento de partículas por medio de proporciones adecuadas de agentes reductores y protectores. Se obtuvieron dispersiones coloidales de nanopartículas, que se evidenciaron por la resonancia de plasmón superficial exhibida en un rango de longitud de onda del espectro radio-magnético de 400 nm a 700 nm, que corresponde desde nanopartículas esféricas a nanoprismas. Además, mostramos la efectividad del extracto de ajo, cuyo componente principal es la alicina, y el extracto de corteza de canela, cuyo componente principal es el cinamaldehído, como agentes reductores y protectores en el proceso de síntesis de nanopartículas. La estabilidad de la dispersión coloidal se extiende por varias semanas. También se evidenció cierta conductividad de nanopartículas de plata incrustadas en películas de pectina. Además se analizó el efecto antibacteriano. La presencia de nanopartículas de plata con diferentes formas se verificó por la señal de resonancia de plasmón superficial detectada por espectroscopía UV, que se corroboró mediante microscopía electrónica de barrido (STEM) y dispersión dinámica de luz (DLS), utilizando el potencial Z para determinar el tamaño de las nanopartículas obtenidas con estas síntesis, además de la morfología de las mismas.

PALABRAS CLAVE

Nanopartículas de plata, morfología de las nanoestructuras, extracto de ajo, resonancia del plasmon superficial (SPR), extracto de corteza de canela, alicina, cinamaldehído.

OUTLOOK

1 INTRODUCTION AND JUSTIFICATION.....	2
1.1 Silver Nanoparticles	3
1.2. Garlic	8
1.3 Cinnamon	9
2 PROBLEM STATEMENT	11
3 OBJECTIVES	12
3.1 General Objective.....	12
3.2 Specific Objectives.....	12
4 METHODOLOGY	13
4.1 Reagents	13
4.2 Materials.....	14
4.3 Equipment	14
4.4 Experimental Description.....	15
4.4.1 AgNPs Synthesis.....	15
4.4.1.1 Chemical Synthesis with Hydrazine (AgNPs-Hydrazine).....	15
4.4.1.2 Chemical Synthesis using Natural Extracts as a Reducing Agent. (AgNPs-Combined).....	16
4.4.1.3 Garlic Extract as a reducing agent (AgNPs-Combined (G))	17
4.4.1.4 Cinnamon Extract as a reducing agent (AgNPs-Combined (C))	18
4.4.1.5 Green Synthesis of AgNPs.....	18
4.4.2 Preparation of conductive polymeric films with AgNPs embeded.....	19
4.4.2.1 PVA-AgNPs-Hydrazine Thin Films	19
4.4.2.2 Pectin-AgNPs-garlic thin Films.....	21

4.4.3 Physicochemical Characterization of the obtained AgNPs	21
4.4.3.1 Evaluation of Surface Plasmon Resonance (SPR) by UV-Vis Spectroscopy	21
4.4.3.2 Determination of size and shape of Nanostructures by Scanning Electron Microscopy (SEM) and Scanning Transmission Electronic Microscopy (STEM)	22
4.4.3.3 Determination of size of AgNPs by Dynamic Light Scattering and e evaluation of the surface potential by measurements of Zeta-Potential	24
4.4.3.4 Analysis by Fourier Transform Infrared (FT-IR)	26
4.4.4 Evaluation of the bactericidal activity of the AgNPs prepared	26
4.4.5 Determination of the Conductive-Impedance of the polymer films prepared with AgNPs	29
5 RESULTS, INTERPRETATION AND DISCUSSION	32
5.1 From Synthesis	32
5.1.1 Chemical Synthesis	32
5.1.2 Combined Synthesis	33
5.1.3 Green Synthesis	34
5.2 Characterization of Silver Nanoparticles obtained.....	36
5.2.1 FT-IR Spectroscopy to the analysis of AgNPs obtained by Green Synthesis	36
5.2.1.1 FT-IR Spectroscopy of AgNPs-Cinnamon	36
5.2.1.2 FT-IR Spectroscopy of AgNPs-Garlic	38
5.2.2 Evaluation of Surface Plasmon Resonance using UV-Vis Spectroscopy	40
5.2.2.1 UV-Vis of AgNPs-Hydrazine.....	40
5.2.2.2 UV-Vis Spectroscopy of AgNPs-Combined.....	42
5.2.2.3 UV-Vis Spectroscopy of AgNPs-Green.....	43
5.2.3 Evaluation of the size and shape of Nanostructures using Electron Microscopy.....	45

5.2.4 Evaluation by Dynamic Light Scattering (DLS) and by Z-potential of AgNPs obtained	49
5.2.4.1 DLS of AgNPs obtained by Green Synthesis	49
5.2.4.2 DLS of AgNPs-Hydrazine	52
5.3 For the applications	52
5.3.1 Electrochemical Impedance Analysis of the polymer with AgNPs	52
6 CONCLUSIONS AND RECOMENDATIONS	60
7 BIBLIOGRAPHY	61

1. INTRODUCTION AND JUSTIFICATION

Currently there has been a growing interest in Nanoscience (and Nanotechnology) that includes a set of scientific and technological disciplines such as novel materials design, pharmaceuticals, textile and food industry, catalysis, among others. These disciplines are oriented to the study and manipulation of systems at the nanoscopic scale and in the study and exploitation of the peculiar behavior that these systems exhibit, not observed at the macroscopic level.

Nanotechnology involves the design, production and application of structures, materials and systems through the control of the shape and size at the nanometer level¹. The word "nano" is a Greek term that refers to something extremely small and is used to indicate one billionth of a meter. Measurements at this length scale allow to work and manipulate the molecular structures. The development of Nanoscience and Nanotechnology come from the proposals of Richard Feynman, Nobel Prize in Physics 1965, who is known as the father of Nanoscience although he did not precisely coin that term. Through his famous lecture "There's a Plenty of Room at the Bottom"² in 1959 he released his ideas about the possibility and importance to study the matter at very small length scale. In this conference given at the annual American Physical Society meeting at California Institute of Technology (Caltech), he introduced the idea of a future in which micro-machines could exist and things will be built at the atomic level. With these proposals began the advance of a new field of science, where it is possible to study, design, create, synthesize and apply functional materials through the control of the its formation.

Nanomaterials can be produced from physical and chemical methods. The first one implies the destruction of sample modulating shape and size of the nanostructure, while the chemical method implies the use of appropriate chemical substances and compounds. Depending on the formation mechanism involved different shapes such as spheres, rods, wires, prisms, can result, and depending on the composition of the substances involved, the several types of material can be classified in:

Carbon-based materials: Macromolecules, proteins, micelles, vesicles, dendrimers, semiconductors and polymeric materials³

Inorganic Nanostructures: Metallic solids structures, metal oxides or metal based compounds.

The use of these nanomaterials has been extended to several industrial fields, and in the last decades, it has contributed to the development of the society through of improve and optimize the technology by the use of nanomaterials in agriculture, transport, food, textile, cosmetics, drugs, communication devices, information storage, among other⁴.

Among the all the possible nanomaterials to be obtained, the metal particles at nanometric level shows optical, electronic, catalytic, magnetic, biological properties, etc., which strongly depend on the size, shape, composition, and structure of the particle⁵. The cause of this peculiar behavior is the large surface/volume ratio exhibited, which concatenate in a great superficial energy, due to the large number of surface atoms. These features generate convenient systems because to their peculiar optical, electronic, magnetic and catalytic properties, which in general are related to its shape, size, composition, crystallinity and particle structure.

The interesting properties exhibited, mainly optical ones, depend on the strong interaction of metal nanoparticles with light, which is caused by the conduction electrons on the metal surface undergoing collective oscillation when excited by light at specific wavelengths, known as Surface Plasmon Resonance (SPR). This oscillation produces unusually strong absorption and dispersion properties⁶ whose frequencies of SPR appear in the UV-Visible wave range. Due to this, the colloidal suspensions of nanoparticles of noble metals, mainly gold and silver, present a strong SPR effect, which generates suspension of different colors, absent in their homogeneous phase (or bulk phase) and in their individual atoms.

1.1 SILVER NANOPARTICLES (AgNPs).

The silver element (Ag) has atomic number 47, its most common oxidation state is +1. However, it can also be found as +2 (example: in AgF_2 - silver difluoride) and +3 (in KAgF_4 – tetrafluoride argenate of potassium). The crystalline structure of silver is FCC faced centered cubic. The various states of the silver are either as salts, metallic particles, nanoparticles, etc, in each case presenting interesting properties.

Of metal nanoparticles, one of which has had the greatest interest in its study and that have a lot of applications are silver nanoparticles. These nanoparticles have peculiar biological, optical, magnetic, electronic and catalytic, thermal properties, which have allowed them to be the most used in commercial products ranging from photovoltaic

sensors to biological and chemical sensors. Also, due to their high electrical conductivity and stability and low sintering temperatures they are used as conductive pastes and fillers. On the other hand, the AgNPs have an especially strong SPR, which implies that they are extremely efficient to absorb and disperse light, and unlike other dyes and pigments, have a color that depends on the size and shape of the particle⁶. Other applications that take advantage of these optical properties is that they are photonic devices, and that they can act as a functional component in several sensors for molecular diagnostics.

Antibacterial activity is one of the most known and commercially exploited applications, such as household items and several medical products. A scheme of the principal medical applications is shown in the Figure 1. For example there are antimicrobial coatings, wound dressings, biomedical devices⁷.

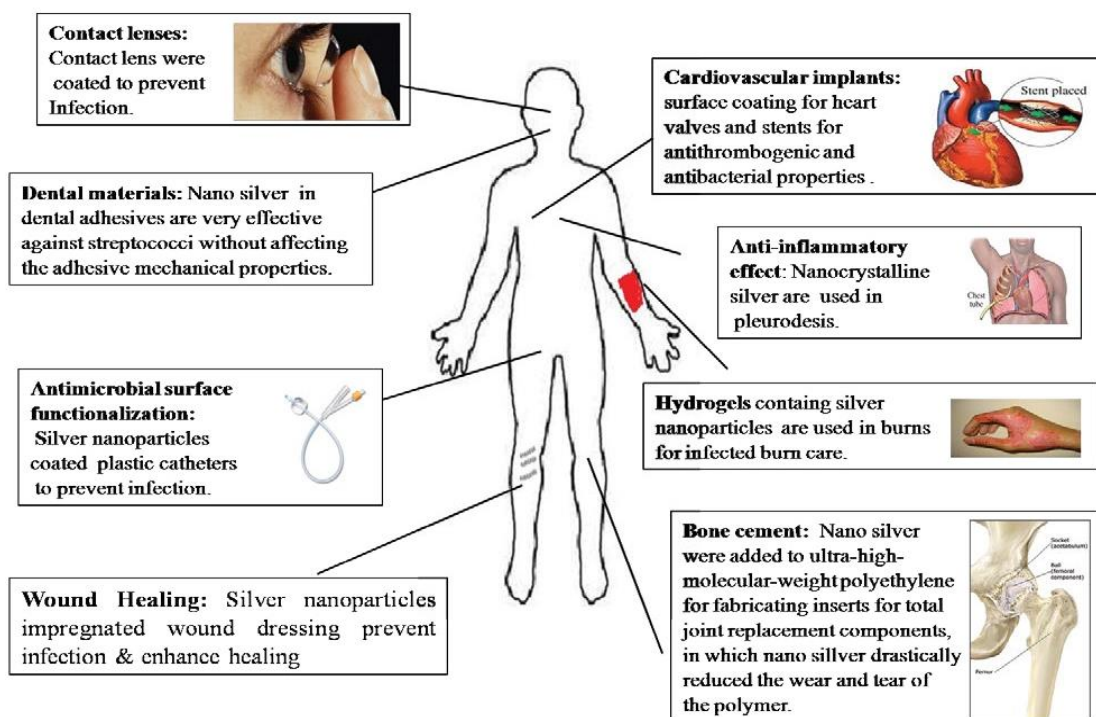


Figure 1. Applications of Silver Nanoparticles Khatoon et al. (2017)⁷.

There are several methods for obtaining nanoparticles from which the most convenient one depends on the further application. Their preparation can be carried out by top-down and bottom-up methods. The first ones are mostly physical or mechanical processes, such as mechanical / ball milling, thermal / laser ablation, sputtering, and in addition to chemical etching. While the bottom-up methods refer to the construction of nanostructures from solutions of their constituent compounds. Among this are: chemical

/ electrochemical precipitation, co-precipitation vapor deposition (CVD), atomic / molecular condensation, sol-gel processes, spray pyrolysis, laser pyrolysis, aerosol pyrolysis⁸.

Although silver nanoparticles, and the other metal nanoparticles, can be obtained by a wide variety of methods, the coprecipitation is one of the most widely used methods. Cushing (2004)⁹ described it, suggesting that it has three stages that are nucleation, growth, and coarsening that govern the particle size, and has the following characteristics:

- The products of the precipitation reaction are poorly soluble and they are formed under supersaturation conditions, such are reached by addition of the reactant or a vigorous stirring speed.
- There are many ways to induce precipitation, and for the synthesis of nanoparticles the most common one is by chemical reactions, for example, reaction of addition, exchange, photo reduction, chemical reduction, oxidation and hydrolysis.
- Nucleation is the key to the precipitation process.
- The precipitation of metals is generally given by the chemical reduction of a metal cation, for this a reducing agent is required, among the most common are H₂, NaBH₄, hydrazine, hydrazine dichloride.
- Secondary processes, such as Ostwald Ripening and aggregation, could dramatically affect the morphology, size and particle size distribution; also properties of the products.

Each one of the stages proposed by Cushing are briefly described as follow:

Nucleation: Like all precipitation process starts with a supersaturated solution. When the precipitation takes place initially numerous small crystallites are formed, this is what is known as the nucleation process.

Growth: The small crystallites formed in nucleation tend to aggregate with each other rapidly to form larger crystals, thermodynamically more stable particles. The growth process can be diffusion-limited or reaction-limited. However, experimentally it has been shown that they are generally diffusion-limited⁹. The growth rate is determined by factors such as concentration and temperature gradients, while new material is delivered to the surface of the particle through long distance mass transfer.

Ostwald Ripening (Coarsening): “It is the phenomenon by which smaller particles are essentially consumed by larger particles during the growth process”⁹.
 Growth termination and NP stabilization.

In the synthesis process it is necessary to use a stabilizer agent to avoid the agglomeration of small particles precipitated from the solution, which can occur at any moment of the synthesis. There are two ways to stabilize nanoparticles:

- By steric repulsion between particles caused by surfactants, polymers, or other organic species bound to the nanoparticle surfaces (generically referred to as capping ligands).
- Electrostatic (van der Waals) repulsions resulting from the chemisorption of charged species (usually, though not necessarily, H^+ or OH^-) at the surfaces.

One of the methods for the synthesis of nanoparticles is the called Green Synthesis, through which the nanoparticles are formed by the use of bio-molecules, and under room temperature and neutral pH. The Green Synthesis also offer a convenient way to obtain nanostructures, although is not a completely and efficient method, as the case of conventional methods, has the benefit of a low environment impact. Also, it is a way to exploit the natural resource coming from the agriculture, and even domestic food, wastes. For the Green Synthesis of silver nanoparticles plant extracts are generally used as reducing agents and a silver salt, such as silver nitrate, as the only other reactant. Several extracts have been tested and have had favorable results, as indicated in the Table 1⁷.

Due to several factors such as its geographic location, geological characteristics, climatic precipitation and temperature, biological and evolutionary factors, Ecuador is one of the most mega-diverse countries on the planet. The combination of all these factors results in different kinds of vegetation in Ecuador¹⁰. An advantage of this varied vegetation is that it can be found endemic plants, as well as others that have been entered into the country, being adapted to different local climates and excellently developed. Such is the case of garlic and cinnamon plants, which have interesting properties that among their many benefits can be used as reducing agents in the synthesis of silver nanoparticles.

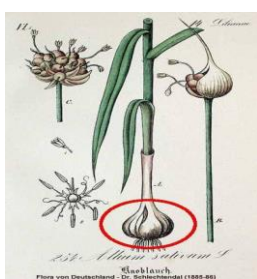
Table 1 Green Synthesis of Silver Nanoparticles by different researches using plant extracts taken Ahmed et al., (2016).¹¹

Plants	Size (nm)	Plant's part	Shape
<i>Alternanthera dentate</i>	50–100	Leaves	Spherical
<i>Acorus calamus</i>	31.83	Rhizome	Spherical
<i>Boerhaavia diffusa</i>	25	Whole plant	Spherical
<i>Tea extract</i>	20–90	Leaves	Spherical
<i>Tribulus terrestris</i>	16–28	Fruit	Spherical
<i>Cococus nucifera</i>	22	Inflorescence	Spherical
<i>Abutilon indicum</i>	7–17	Leaves	Spherical
<i>Pistacia atlantica</i>	10–50	Seeds	Spherical
<i>Ziziphora tenuior</i>	8–40	Leaves	Spherical
<i>Ficus carica</i>	13	Leaves	-
<i>Cymbopogan citratus</i>	32	Leaves	-
<i>Acalypha indica</i>	0.5	Leaves	-
<i>Premna herbacea</i>	10–30	Leaves	Spherical
<i>Calotropis procera</i>	19–45	Plant	Spherical
<i>Centella asiatica</i>	30–50	Leaves	Spherical
<i>Argyreia nervosa</i>	20–50	Seeds	-
<i>Psoralea corylifolia</i>	100–110	Seeds	-
<i>Brassica rapa</i>	16.4	Leaves	-
<i>Coccinia indica</i>	10–20	Leaves	-
<i>Vitex negundo</i>	5 & 10–30	Leaves	Spherical & fcc
<i>Melia dubia</i>	35	Leaves	Spherical
<i>Portulaca oleracea</i>	<60	Leaves	-
<i>Thevetia peruviana</i>	10–30	Latex	Spherical
<i>Pogostemon benghalensis</i>	>80	Leaves	-
<i>Trachyspermum ammi</i>	87- 99.8	Seeds	-
<i>Swietenia mahogany</i>	50	Leaves	-
<i>Musa paradisiacal</i>	20	Peel	-
<i>Moringa oleifera</i>	57	Leaves	-
<i>Garcinia mangostana</i>	35	Leaves	-
<i>Eclipta prostrate</i>	35–60	Leaves	Triangles / pentagons / hexagons
<i>Nelumbo nucifera</i>	25–80	Leaves	Spherical / triangular
<i>Acalypha indica</i>	20–30	Leaves	Spherical
<i>Allium sativum</i>	4–22	Leaves	Spherical
<i>Aloe vera</i>	50–350	Leaves	Spherical / triangular
<i>Citrus sinensis</i>	10–35	Peel	Spherical
<i>Eucalyptus hybrid</i>	50–150	Peel	-
<i>Memecylon edule</i>	20–50	Leaves	Triangular / circular / hexagonal
<i>Nelumbo nucifera</i>	25–80	Leaves	Spherical / triangular
<i>Datura metel</i>	16–40	Leaves	Quasilinear superstructures
<i>Carica papaya</i>	25–50	Leaves	-
<i>Vitis vinifera</i>	30–40	Fruit	-

1.2 GARLIC

Garlic is an herbaceous plant, belonging to the Alliaceae, characterized by growing in a bulb of up to 20 teeth or more. Garlic has important crops in Ecuador mainly in the Sierra region, because the requirements of cold temperate climates in its early stages of formation, and of higher temperature in its later stages, which are presented in the provinces of Chimborazo, Carchi, Tungurahua, Cotopaxi, Azuay, Cañar and Loja.

In the *Table 2* is shown a brief taxonomic description of the plant.



Family	<i>Liliaceae</i>
Subfam	<i>Allioideae</i>
Scientific name	<i>Allium sativum</i> L
Gender	<i>Allium</i>
Plant	Bulbous, vivacious and rustic

Table 2 Taxonomic description of the Garlic.

The active principle of garlic extract is allicin, shown in the Figure 2, which is a very interesting sulfur molecule to which all the benefits offered by garlic are attributed. For example its antibiotic and antiviral effect or its ability to improve blood pressure¹² when consuming high doses, and its antioxidant effect¹³ (the most important in this project). The allicin is obtained from the hydrolysis (for the air humidity) of alliin, being the pyruvic acid the other product of the reaction, as can be seen in the Figure 3.

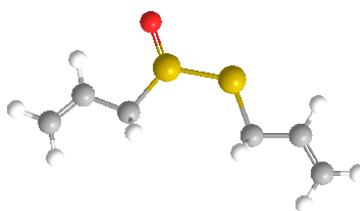


Figure 2 Allicin Molecule. (Carbon atoms-gray spheres, Hydrogen atoms-white spheres, Sulfur atoms-yellow spheres and oxygen atom red sphere)

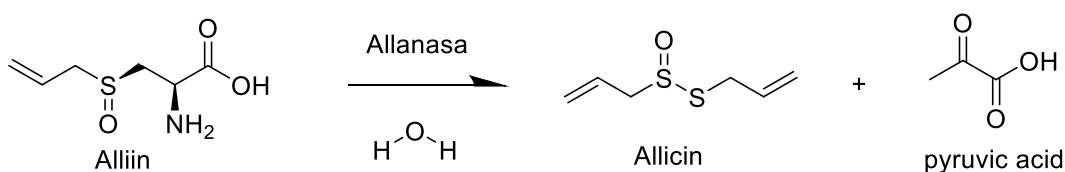


Figure 3 Chemical Reaction for the Allicin formation.

In the next *Table 3*, information is added of some garlic components to which certain biological activities are attributed.¹³

Table 3 Principal components of garlic with the biological activity Cordova M. et al; 2010¹³

Component	Biological Activity
Allixina	Antioxidant
Sapponins	Hypertensive
Aliina	Hypertensive
Allicin	Prevents damage to DNA
Ajoeno	Anti-inflammatories
Fructans	Cardioprotectors

1.3 CINNAMON



Table 4 Taxonomic description of *Cinnamomum zeylanicum* .

Kingdom	Plantae
Division	Magnoliophyta
Class	Magnoliopsida
Family	Lauraceae
Gender	Cinnamomun
Species	<i>Cinnamomum zeylanicum</i>

The word cinnamon has a French origin, it come from the word Canne whose meaning is pipe or tube, and in diminutive is pronounced cannelle¹⁴. Cinnamon is an ancestral plant native of Sri Lanka (India) and from XVII century was introduced to Latin America and Ecuador, where it is cultivated in the Amazonian region. It is a hardy plant that can grow in all types of low soil and varied tropical conditions. The bark is the part of the cinnamon widely used and studied¹⁵. The Table 4, and Table 5 contain important information about the taxonomy and composition of cinnamon.

Table 5 Active principles of cinnamon bark. Aizaga et al., (2017)¹⁴

Compound	Percent
Trans-Cinnamic Aldehyde	55- 75%
Eugenol	< 7.5%
Linalool	1.0-6.0%
Beta-Caryophyllene	1.0-4.0%
Cineol	< 3.0%
Trans-2-Methoxycinnamic Aldehyde	0.1-1.0%
Benzyl Benzoate	< 1.0%
Coumarin	< 0.5%
Safrole	< 0.5%

The most prominent active principle in cinnamon bark extract is cinnamaldehyde, whose structure is shown in the Figure 4 .This molecule is an aldehyde that is suggested to have a reducing effect on silver. This premise is made due to the knowledge of the Tollens's Test¹⁶.

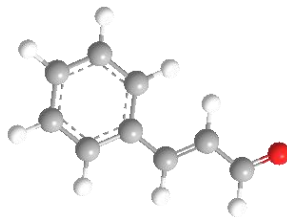


Figure 4 Structure of Cinnamaldehyde molecule. (Gray spheres-Carbon atoms, Hydrogen-white spheres and oxygen atom-red sphere)

The Tollens's test is a laboratory procedure to distinguish an aldehyde from a ketone: a mild oxidizing agent (silver complex) is mixed with an unknown aldehyde or ketone; if the compound is oxidized, the presence of an aldehyde is identified, if a reaction does not occur, it is a ketone¹⁶.

These two molecules, allicin and cinnamaldehyde are potential reducing agents for the synthesis of silver nanoparticles, and can allow a performance of Green Chemistry because it can reduce or eliminate the use of expensive chemicals. And with the advantage of using products from biomass, which can be waste from agriculture that as mentioned is very rich in Ecuador.

2. PROBLEM STATEMENT

The controlled synthesis of nanoparticles is one of the topics of interest in the study of nanotechnology, through which it is possible to modulate their size and/or morphology, and this conditions its specific use in subsequent applications. However, the most common methods involve the use of toxic chemical compounds, among which it can be mentioned reducing agents, such as hydrazine and sodium borohydride, whose descriptions can be seen in the Table 6. They are key compounds in the synthesis of nanoparticles, however, could be the cause of the toxicity that the AgNPs may have, or in turn the synthesis may release by-products. Another problem with these compounds are undoubtedly the costs and processes for obtain them.

One of the clean alternatives will always be Green Chemistry, which has as its principle the design of products or processes that reduce or eliminate the use of polluting products from¹⁷. Also, it is intended to take advantage of the benefits of belonging in a mega-diverse country like Ecuador and work with products that are easy to access, even for adding value to certain agriculture waste products.

3. OBJECTIVES

3.1 General Objective:

To synthesize and characterize silver nanoparticles using as reducing and capping agents biocompatible molecules as allicin from garlic extract and cinnamaldehyde from cinnamon bark extract.

3.2 Specific Objectives

1. To control the size and morphology of silver nanoparticles by use of suitable proportions of the different agents involved in the processes of synthesis.
2. Synthesize AgNPs by Green Synthesis using garlic and cinnamon bark extracts to evaluate their reducing and capping effects in the synthesis of nanoparticles.
3. To evaluate the effect of kind of reducing agent on the size and morphology of AgNPs.
4. Characterize the obtained AgNPs and evidence some of their properties for possible applications, for example, as in the preparation of conductor polymer.
5. To evaluate the antibacterial effect of AgNPs synthesized.

4. METHODOLOGY

4.1 Reagents

Reagents are acquired from different commercial industry, for example:





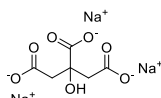


Sigma Aldrich: Silver Nitrate (AgNO_3) G.A., Sodium Borohydride (NaBH_4) G.A., Hydrazine (N_2H_4) G.A., Ammonium Chloride (NH_4Cl) G.A., Propylene Carbonate (G.A.), Sodium Citrate (G.A.), Hydrochloric Acid (G.A.),

LobaChem: Poly Vinyl Alcohol (PVA) (G.A.).

Pectin and Ethanol (99%).

The extracts are obtained from respective raw materials brought in local stores. The most important properties of the used reagents are given in the Table 6.

Table 6. Physical and chemical properties of reagents used in the synthesis and analysis of silver nanoparticles.

Compound	Purity	M. Weight [g/mol]	Density [g/cm ³]	Boiling P. [°C]	Melting P. [°C]	Hazards Statements
Silver nitrate (AgNO_3)	~99.5%	169.87	4.35	444	212	
Sodium borohydride (NaBH_4)	96%	37.83	1.07	NA	360	
Hydrazine (N_2H_4)	35%	32.04	1.028	-57	117.2	
Ammonium Chloride (NH_4Cl)	~99.5%	53.49	N/A	N/A	340	
Chlorohydric acid (HCl)	38%	55.55	1.18	57	-35	
Pectin 	N/A	194.043	N/A	142	N/A	N/A
Ethanol ($\text{C}_2\text{H}_5\text{OH}$)	99.8%	46.07	78	-114	0.785	
Sodium Citrate 	~99.5%	258.06	N/A	300	1.7	
PVA ($\text{C}_2\text{H}_4\text{O}$) _x	88%	44.03	228	200	1.19	

4.2 Materials

Table 7 Material used during the development of the synthesis and evaluation of silver nanoparticles.

Volumetric Pipettes	1 mL, 3mL, 5 mL	Magnetic stir Tweezers Laboratory handle Spatula Bunsen lighter Stir bar Droppers Soxhlet Equipment Steam Distillation equipment Thermometer
Burette	10 mL	
Beakers	10 mL 50 mL 100 mL	
Plastic Petri dishes	5 cm of diameter	
Volumetric Flask	25 mL, 100 mL	
Round flask	500 mL	
Viales	2 mL, 5 mL	
Kitasate	500 mL	
Cilinder graduated	10 mL 50 mL 100 mL	
Filter Paper		

4.3 Equipment.

Table 8 Equipment used for the synthesis and characterization of silver nanoparticles

For the synthesis:	
Analytical Balance:	Cobos / precision 152g/ 0.1 mg (SAVAIN)
Electric Oven	POL-EKO apertura SP.J SLW115 STD
Hot / Magnetic Plate.	VELP. Scientifica AREC. T
Vacuum system filtration.	
For the characterization / analysis:	
FT-IR:	Perkin Elmer / 100 FT-IR Spectrophotometer
UV-Vis-NIR	Perkin Elmer / LAMBDA 1050 UV/Vis Spectrophotometer (175 to 3300 nm)
SEM	Phenom World / PhenomProX
STEM	FEI Company / Electronic Field Emission Scanning Microscope (FE-SEM). / Nova Nano 200 SEM / Vacuum mode using a STEM I XT detector.
Z-Sizer (Particle Size Analyzer)	
Potenciostat Galvanostat	Metrohm / Autolab B.V. AUT87041
UV-lamp with wavelength	

4.4 Experimental Description

4.4.1 AgNPs Synthesis

For the synthesis of silver nanoparticles by the Chemical and Green methods, 1mM and 3mM silver nitrate solutions were prepared, using distilled water as solvent. Different methods of synthesis were tested, they are referred as: Chemical Synthesis with Hydrazine, Combined Synthesis using natural extract as reducing agent, and Green Synthesis. All of them were focused in bottom up methods for which were used different chemical compounds acting as metal source, reducing and capping agents.

4.4.1.1 Chemical Synthesis with hydrazine (AgNPs-Hydrazine)

The chemical synthesis of AgNPs was based on the protocol described by A.C. Power and S. Byrne¹⁸. This bottom up method consisted in different stages, which are briefly described:

Preparation of Seed Suspension:

- Silver nitrate solution 3mM was added to a sodium citrate solution 2.5mM, in a proportion 1:1 ($v_{\text{Ag}^+} : v_{\text{citrate}}$) with stir by a magnetic plate.
- Drop by drop and keeping the stir, 6 mL of a sodium borohydride solution 1 mM was added to 20 mL of the previously prepared solution. By this *Nucleation Process* it was generated a solution denoted as Seed Suspension.

Nanoparticles Formation and Growth:

- 5 mL of a PVA solution 1% was poured in a 50 mL beaker with constant stir. The PVA works as a stabilizing agent.
- Keeping the stir, to the PVA solution was added 1 mL of Seed Solution, 3 mL of sodium citrate solution 1 mM, and 5 mL of a hydrazine solution 0.1 M. The sodium citrate acts as a capping agent, while the hydrazine acts a reducing agent.
- With the help of a burette, it was poured little by little, very slowly, and maintaining a continuous stirring, different amounts of a solution of 1 mM AgNO_3 were added, which produced different colloidal dispersions depending on the amount added. This procedure was corresponding to the nanoparticle *Growth process*.
- Each time that the formed colloidal dispersion changes color, such as those shown in the Figure 5, a sample of 1 mL of it was taken for further analysis.

In an inset of the Figure 5 is indicated the AgNO_3 volume used throughout the identification of samples, for example, AgNPs-H-1 is referred to silver nanoparticles formed after adding 1 mL of 1mM AgNO_3 in presence of hydrazine as reducing agent.

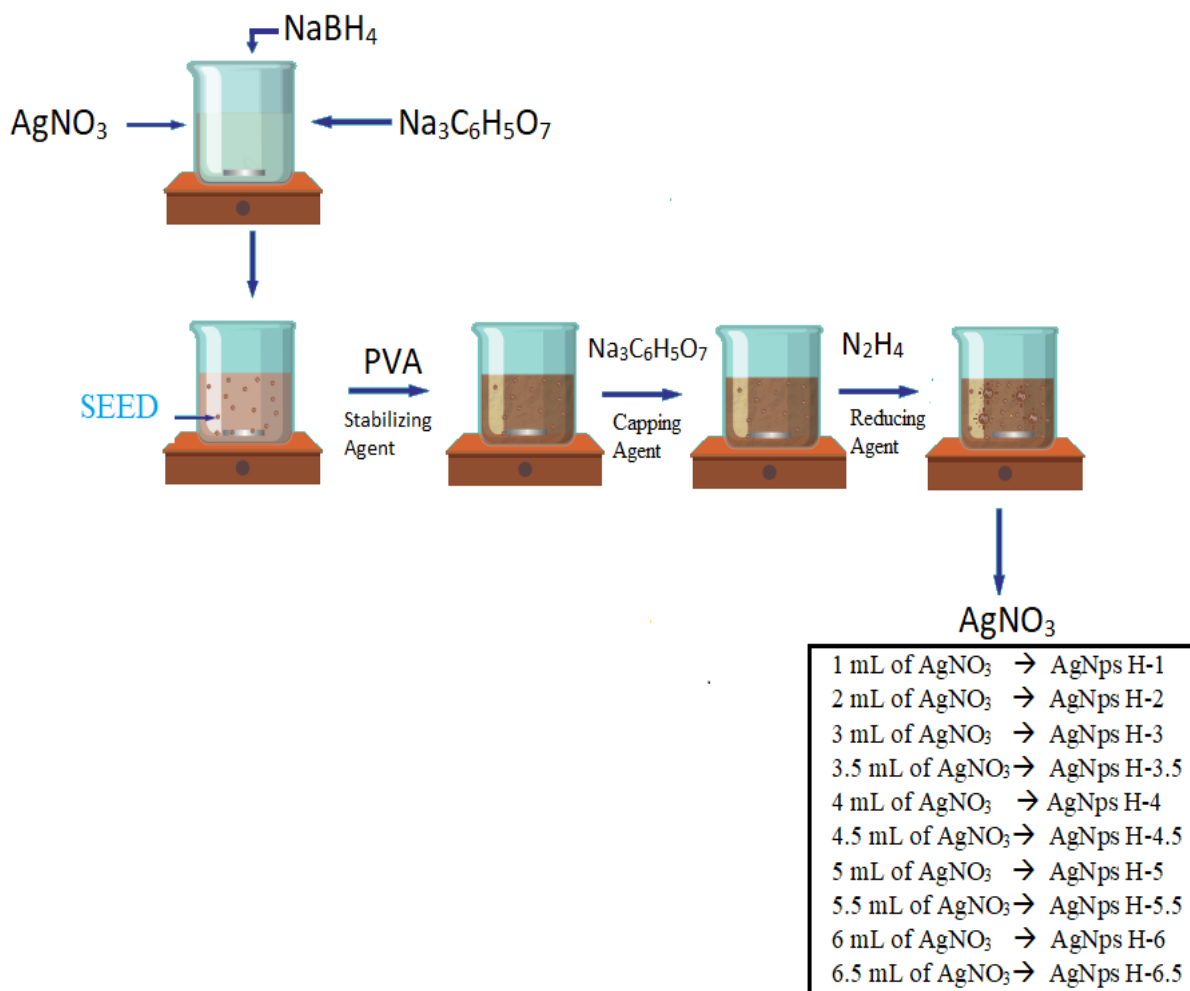


Figure 5 Schematic representation of Chemical Synthesis of AgNPs using hydrazine as reducing agent.

4.4.1.2 Synthesis of AgNPs using Natural Extracts as a Reducing Agent. (AgNPs-Combined)

After having a vast knowledge in the method of Chemical Synthesis of AgNPs, it was proposed to modify the process and turn it into one that is friendlier to the environment, replacing some toxic reagents with some bio-compounds obtained from natural sources. For this, the same Chemical Synthesis procedure was carried out but replacing the hydrazine solution with the Garlic Extract, and other procedure replacing the hydrazine solution with Cinnamon bark Extract.

4.4.1.3 Garlic Extract as a reducing agent (AgNps-Combined (G))

In this case, garlic cloves, ethanol, distilled water and hydrochloric acid solution 0.05% were used¹⁹. Three procedures were carried out simultaneously using different solvents, following the procedure described below:

30 g of peeled garlic cloves were weighed, crushed and placed in 100 mL of solvent. The mixture was boiled for 5 minutes, and then they were allowed to stand for 2 weeks and they filtered under vacuum. As it can see in the Figure 6, the color of the resultant extracts solution was dependent on the solvent, that is:

- *The garlic extract obtained with hydrochloric acid turned blue/green and very dense, which complicated the filtration.*
- *The solution obtained of the extraction with ethanol turned yellow and not very dense, facilitating vacuum filtration.*
- *The garlic extract obtained with water became too dense and almost did not take any different color.*

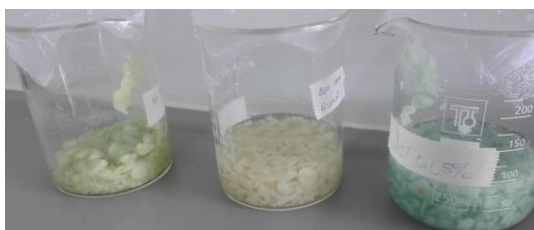


Figure 6 Pictures of the resulting samples of the garlic extraction using different solvents. From left to right: ethanol (green), water (yellow) and chlorohydrin acid.

Due to the physical characteristics observed and the results obtained by FT-IR spectroscopy, it was decided to work with the garlic extracts obtained with ethanol.

The garlic extract was used as a reducing agent, replacing the hydrazine in the protocol described in the Chemical Synthesis section. For that, it was added 2 mL of garlic extract after the addition of sodium citrate, as is indicated in the previous section, during the NP-growth process. In the same way as was described before, were taken different samples of the colloidal suspension obtained after the addition of different volumes of AgNO₃ solution 1 mM for further analysis.

4.4.1.4 Cinnamon Extract as a reducing agent. (AgNPs-Combined (C))

The first step to develop this procedure was the obtaining of cinnamon extract, for which a simple distillation the extraction of cinnamon was carried out as is described:

50 grams of cinnamon bark were crushed in a mortar to form cinnamon barks with smaller size. The cinnamon crushed was placed in a 500 mL round bottom flask with 300-400 mL of distilled water, and a stir bar. Next, the steam distillation apparatus was set up as it is shown in the Figure 7 and the distillation process started using the cinnamon bark moderately crushed. This process lasted approximately 2 hours and a rather dense, colorless solution was obtained.

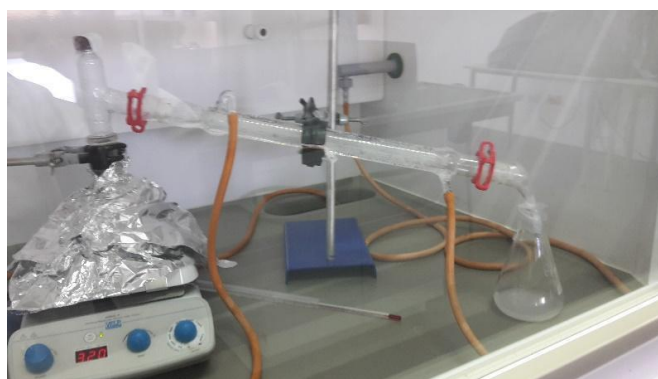


Figure 7 Picture of experimental setup of the steam distillation of bark cinnamon.

In the similar way as was described for the garlic extract case, it was used the cinnamon bark extract as a reducing agent, using of it instead of the hydrazine. After the addition of different volumes of AgNO_3 solution 1 mM were taken different samples of the colloidal dispersion obtained for further analysis for their characterization.

4.4.1.5 Green Synthesis of AgNPs

To check the reducing effect of both the garlic extract and the cinnamon bark extract, a Green Synthesis was developed in which the silver salt and the plant extracts were used.

- For the AgNPs-garlic, 2 mL of garlic extract and 1 mL of 3 mM AgNO_3 were mixed and stirred for approximately 10 minutes. In the Figure 8 is shown a scheme of this synthesis.

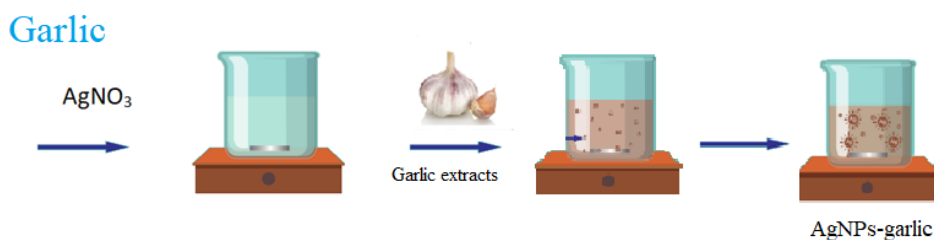


Figure 8 Scheme of Green Synthesis of AgNPs, using garlic as reducing agent.

- For the AgNPs-cinnamon, 3 mL of cinnamon bark extract and 0.5 mL of 10 mM AgNO_3 were placed in a beaker, heated at 40°C for 5 min with stir. The resulting dispersion was characterized for the evidence of the formation of AgNPs. In the Figure 9 is shown a scheme of this synthesis.



Figure 9 Scheme of Green Synthesis of AgNPs using cinnamon as reducing agent

4.4.2 Preparation of conductive polymeric films with AgNPs embedded

In view of the fact that the conductive polymeric films have a wide range of applications, polymer films were prepared from natural and synthetic sources, in which silver nanoparticles were embedded and the effect of the presence of the nanoparticles on the conductivity of the resulting films was evaluated.

Two procedures were carried out for the preparation of these polymers, one using polyvinyl alcohol (PVA) to which was embedded the AgNPs-Hydrazine, and another using pectin and NPs-Ag-garlic, in order to make a completely green treatment.

4.4.2.1 PVA-AgNPs-Hydrazine Thin films

Mixtures of PVA solution and colloidal suspensions of AgNPs-Hydrazine were prepared with the relation PVA-AgNPs-Hydrazine, following the procedure:

- In a 50 mL beaker was poured the amounts of 5% PVA solution and AgNPs-Hydrazine suspensions indicated in the Table 9 identifying them appropriately. This mixture was stirred for 5 min.
- The films formed were removed of the Petri dishes and stored appropriately.
- Once homogenized the mixtures, they was poured into a plastic Petri dish (5 cm of diameter), which were taken to the oven at 50°C for 18 hours to gel.

Table 9 Volumes of AgNps-Hydrazine (VAgNPs), PVA 5% solution (VPVA-5%), and the respective total volume (Vtotal) for the thin films preparation

Colour	Wavelength of maximum of the peak	$V_{\text{NPs-Ag}} / V_{\text{total}}$	$V_{\text{PVA 5\%}} / V_{\text{total}}$
Yellow	415 nm	0.3	0.7
Yellow	445 nm	0.25	0.75
Red	510 nm	0.3	0.7
Purple	567 nm	0.3	0.7
Blue	695 nm	0.3	0.7
Colorless	Blank	0	1

The resulting films are shown in the Figure 10, in which can be noted the different colorations. Each one of color is associated with the wavelength at which the absorbance of radiation due to the SPR phenomenon is maxima, that is, the coloration associated with the colloidal suspension of nanoparticles used for the preparation of the films.



Figure 10 Picture of thin films obtained from PVA with AgNPs-Hydrazine embedded.

4.4.2.2 Pectin-AgNPs-garlic Thin Films

Three thin pectin-based films were prepared varying their composition to modify their conductivity. This was reached using for one case a 0.1 M ammonium chloride (NH₄Cl) solution as a doping agent for pectin, and for another case the doping effect was reached by the use of colloidal suspension of AgNPs-garlic. Both kind of films were compared with that consisting of only pectin²⁰. The conditions for preparation of Pectin-NPs-garlic, indicated in Table 10, were chosen according to the information provided in the literature²¹. To led gelify was required initially to sterilize the samples, for which was needed to irradiate the samples with a radiation of 235 nm using an UV-lamp.

Table 10 Description of the amounts of the mass of pectin and volume of water used in the thin films preparation.

	Pectin	H₂O	Other
Pectin	1.23 g	15 mL	_____
Pectin + NH ₄ Cl	1.23 g	15 mL	0.033 mL NH ₄ Cl
Pectin + NPs-Ag-garlic	1.23 g	14 mL	1 mL NPs-Ag garlic

4.4.3 Physicochemical Characterization of the obtained AgNPs.

The AgNPs formation was evidenced by the analysis of samples of colloidal systems obtained by different characterization techniques. These analyses allowed the evaluation of some of their morphological and chemical features.

4.4.3.1 Evaluation of Surface Plasmon Resonance by UV-Vis Spectroscopy

The presence of free electrons in the conduction band of metal nanoparticles (electrons in d orbital in a Ag atom) interact with an external electromagnetic field, as for example an incident light beam with a larger wavelength than that the nanoparticles, causing a strong interaction between both nanoparticle and light beam. The light in resonance with the oscillation of the plasmon located near the surface causes the free electrons in the metal to oscillate. That is, the conduction electrons move collectively to detect the distribution of charge perturbed in the oscillation of the plasmon. As the wave front of the light passes the electron density in the particle is polarized on a surface and

oscillates in resonance with the frequency of the light causing a permanent oscillation²². This phenomenon is known as Surface Plasmon Resonance, and a representation of it is shown in the Figure 11.

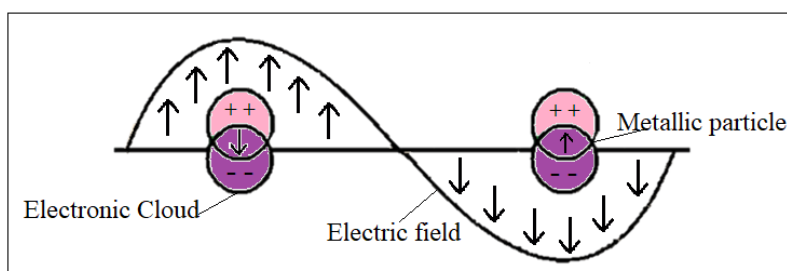


Figure 11 Representation of the Surface Plasmon Resonance (SPR) phenomenon of metal nanoparticles.

As the shape or size of the nanoparticle varies, the geometry of the surface changes causing an increase in the density of the electric field on the surface. This causes a change in the oscillation frequency of the electrons, generating different cross sections for the optical properties, including absorption and dispersion²². It is because of this that this phenomenon is widely used in the morphological characterization of metal nanoparticles²³, distinguishing the metal element constituent due to that each one of them absorbs at different wavelength. For example, the optical extinction spectrum of a colloidal dispersion of silver nanosphere to presents a band in the proximity of 445 nm scattering the blue light with a scattering cross-section of $3 \times 10^{-2} \mu\text{m}^2$, while for the gold nanoparticles the band in the proximity of 520 nm²⁴.

For carry out the SPR analysis for silver nanoparticles obtained in this project was used an UV-Vis-Near IR spectrometer, analyzing a range of wavelength between 300 nm and 800 nm, for which was used a quartz cuvette.

4.4.3.2. Determination of size and shape of Nanostructures by Scanning Electron Microscopy (SEM).

In general, *Electron Microscopy* is a characterization technique of materials, which uses an electron beam to examine objects on a very fine scale. On one hand, the *Transmission Electron Microscopy* (TEM) allows a study of internal structures, and their signals are based on several phenomena that are generated during the inelastic interactions of the electrons with the sample. On the other hand, the *Scanning Electron*

Microscopy (SEM) is a very versatile technique, which serves for the characterization of microstructure, morphology and composition of samples. SEM is used to visualize the surface of objects. The sample to be analyzed must be conductive, otherwise it is required a base, on which the sample is placed, such as graphite or a metal thin layer like gold or aluminum, to provides the necessary conductive character²⁵. The equipment for this microscopies has some differences described in Figure 12.

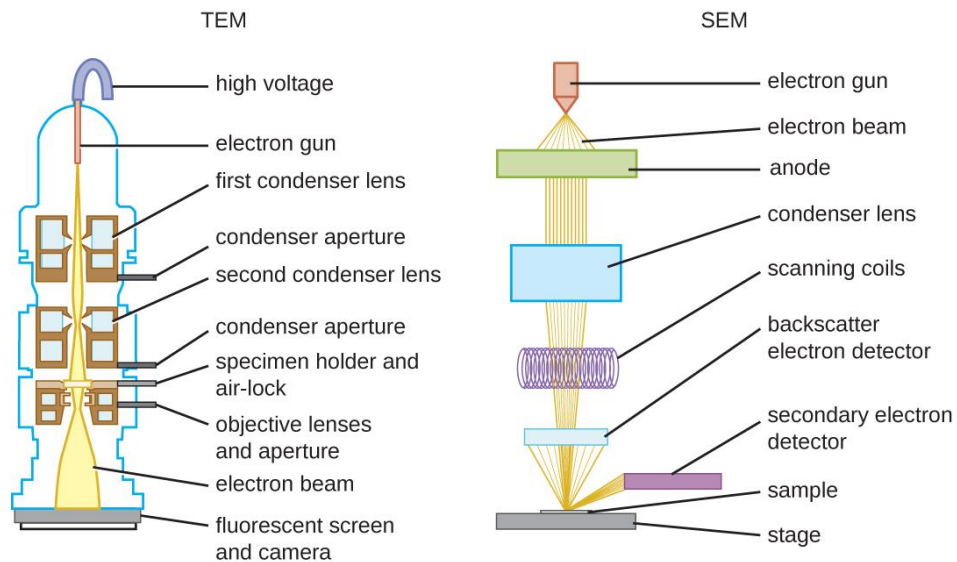


Figure 12 Schematic representation of differences between TEM and SEM microscopies taken from CNX OpenStax 2016

The electrons are accelerated by a potential difference that can range from 50 to 30,000 volts, in order to take advantage of the wave behavior of them, taking place their acceleration in the microscope column. The accelerated electrons travel through a cannon and focus through the condenser and objective lenses, where the image of the filament is reduced so that the electron beam becomes as small as possible. This thin beam of electrons is swept over the sample point by point.

The image formation in SEM corresponds to signals produced by the interactions of the atoms of the sample with the beam of electrons that have impinged on the sample. These interactions are of elastic type (the energy that the electrons lose when colliding with the sample can make other electrons go off and produce X-ray secondary electrons), and inelastic (electrons that bounce like billiard balls). Due to its high resolution and high image speed, both SEM and TEM are the standard methods for direct imaging and dimensional measurements of micro and nanostructures.

The STEM technique combines the principles of TEM and SEM microscopies, and just like SEM, it is slid a thin beam of electrons around the sample. The immersed interactions between the beam and the atoms of the sample generate a flow of signals that serve to form a virtual image. The STEM technique allows an improvement in spatial resolution, which is an advantage over conventional SEM. As in TEM, STEM requires very fine samples and mainly detects the electrons transmitted through a specimen, and its advantage over TEM is that it allows the use of other signals that do not need to be spatially correlated in TEM, such as secondary electrons, scattered electrons, characteristic X-rays, and energy losses of electrons²⁶.

The characterization by STEM was performed in the “Centro de Investigación de Materiales Avanzados” (CIMAV) in Monterrey City – Mexico using the equipment Scanning Electronic Microscope (FE-SEM) model Nova Nano 200 SEM. The samples analyzed were AgNPs-H3.5, AgNPs-H5, AgNPs-H8, AgNPs-garlic, and AgNPs-cinnamon. Each one of the samples for the analysis were prepared as follows:

- *3 drops of the sample were dispersed in 2 mL of isopropanol. Subsequently, this mixture was subjected to an ultrasound bath for 5 minutes in order to disperse the particles.*
- *A drop of such dispersion was taken and placed on a Lacey Carbon Type-A copper grid (300 mesh), and then was allowed to dry at room temperature.*

4.4.3.4 Determination of size of AgNPs by Dynamic Light Scattering and evaluation of the surface potential by measurements of Zeta-Potential.

The Dynamic Light Scattering (DLS) is the technique mostly used to determine dimensions of nanoparticles, and the measurements are carried out from the suspended particles in a liquid phase. This technique uses the temporal variation of the scattered light of the suspended particles exhibiting a Brownian motion, which leads to its hydrodynamic size distribution. Brownian motion is the random movement of particles caused by the incessant collisions of the solvent molecules that surround them²⁷. Brownian motion will be slow the larger the particle, so, the smaller particles are "expelled" by the solvent molecules and move more quickly. For this analysis, a known high precision temperature is required because that the knowledge of the viscosity is necessary. This temperature must also be stable, if not, the convection currents in the

sample will cause non-random movements that will ruin the correct interpretation of the size.

The speed of Brownian motion is related with a property known as the *diffusion coefficient of translation*, which in turn is related with the diameter of particle through the Stokes-Einstein equation. The obtaining values are correspondents to Hydrodynamic diameter and the equation are describe in (eq d1):

$$dH = \frac{k_B T}{3D\pi\eta}, \quad (\text{eq d1})$$

where the term dH is referred to the hydrodynamic diameter of nanoparticle with a translational diffusion coefficient D immerse in a medium of viscosity η . k_B and T have the usual mean of Boltzmann constant and absolute temperature.

The equipment used for determination of the diameter of the nanoparticle is also used to evaluate the *Z-potential*, which is referred to the electrical potential on the surface of the nanoparticle. The colloidal particles dispersed in a suspension having ionic and bipolar characteristics are electrically charged, for this reason the evaluation of the *Z-potential* is a very useful technique for evaluating the nanoparticles since it describes the intensity of the static electric field of the double layer at the boundary between the particle and the liquid phase. The values obtained are closely related to the stability of the suspension and the morphology of the surface of the particles²⁷.

The analysis was performed in Ecocampus in the Benemérita Universidad Autónoma de Puebla in Puebla-Mexico. The samples used for this characterization were AgNPs-garlic, AgNPs-cinnamon, AgNPs-H-3.5, AgNPs-H-5, and AgNPs-H-8. The experimental method for this analysis consisted in to pour the sample of silver nanoparticles in a quartz cuvette that then was introduced in the DLS equipment. For an optimal analysis it is needed to know the medium in which the AgNPs are dissolved, for this particular case the AgNPs are dissolved in an aqueous medium, for which it have to include the next information suggested in the database of the equipment:

Refractive index for silver → RI: 1.333

Viscosity → η : 0.8772 cP

When it is analyzed other lesser-known material, it is necessary to look the related information for that in the literature.

4.4.3.5 Analysis by Fourier Transform Infrared (FT-IR)

Through the analysis by FTIR it could be possible to distinguish the small absorption bands of functionally active residues, as sodium citrate, or extracts, from that of the large absorption of the entire molecules. This difference in the absorption would allow knowing whether the citrate or the bio-molecules are involved in the mechanism of synthesis of nanoparticles. Furthermore, because the FTIR is a non-invasive technique, it could lead to study of confirmation of functional molecules covalently grafted onto silver nanostructures.

The samples of garlic and cinnamon bark extracts were characterized by FT-IR in the Escuela Politécnica del Litoral (ESPOL), located in Guayaquil-Ecuador, in the Centro de Investigación y Desarrollo de Nanotecnología. (CIDNA), and their analysis was carried out with *SpectraGryph* software.

4.4.4. Evaluation of the bactericidal activity of the AgNPs prepared.

One of the peculiar properties of AgNPs, is they present bactericidal activity and therefore they have been used for several biomedical applications, including as antibacterial agents. The antibacterial activity of the AgNPs has been widely studied and its effect depends, among other properties, on their size²⁸, being the of smaller sizes that with greater activity. In that case, the nanoparticles have more surface available for interaction with the surface of the bacterial membrane, which it could generate an alteration of some primary functions such as permeability and respiration²⁹, causing the death of the bacteria.

The evaluation of the antibacterial activity of the AgNPs prepared was carried out in the Laboratorio de Microbiología Hospitalaria y de la Comunidad in the Instituto de Ciencias of the Universidad Autónoma de Puebla (LMHyC - ICUAP - BUAP, by its initials in Spanish). The researcher collaborators proposed the *Kirby-Bauer Method* for this study, which was performed for colloidal suspensions of AgNPs with different concentrations. Three repetitions for each concentration were made, testing eight different kinds of bacteria.

The method of *Kirby-Bauer Method* is widely used to determine the sensitivity of a microbial agent against an antibiotic, and consists in inoculating a standard quantity of microorganisms on a plate with the Muller Hinton culture medium, called agar, forming

a bacterial turf. The antibiotic system was placed in a sensidisk prepared from filter paper. The halo formed around the disc, called zone of inhibition, is an indication of the inhibition of microorganism growth due to the diffusion of the antibiotic from the disc to the agar. This halo was measured and compared with standard antibiotics behavior³⁰.

The 1 mM and 3mM AgNO₃ solutions, and the garlic and the cinnamon extracts, with the same concentrations as the testing samples, were tested and evaluated their bactericidal activity and used as blanks of sample. Also, the control solution was prepared mixing polyvinyl alcohol (PVA), sodium citrate, sodium borohydride, and hydrazine, which were presented in the same mixture as the AgNPs, but without AgNO₃. The Mueller-Hinton broth base (MHB) is used.

The different kinds of bacteria with which was tested the bactericidal activity of the AgNPs prepared are listed in the Table 11.

Table 11 Kinds of bacteria used in Kirby Bauer analysis

Resistant using with AgNPs-Green	Sensitive using with AgNPs-Hydrazine
PE52 (Pseudomonas)	PAO1 (Pseudomonas aeruginosa)
AN54 (Acinetobacter haemolyticus)	AN2 (Acinetobacter)
C7230 (E. coli)	E.coli DH5α
29213 (Staphylococcus aureus)	29213 (Staphylococcus aureus)

The samples evaluated correspond to AgNPs-Garlic, AgNPs-Cinnamon, AgNPs-H1, AgNPs-H3.5, AgNPs-H5, AgNPs-H8, remembering that these last fourth samples correspond to nanoparticles prepared using hydrazine as reducing agent, being the final number in their codes the volume of 1 mM AgNO₃ used for their preparation, as is mentioned below, and the resulting nanoparticles to present the mainly the shape indicated. The experimental methodology followed for this analysis consisted in:

1. Samples selection, implying the nanoparticles prepared from natural extracts and those using hydrazine:

AgNPs-garlic: Color light brown.

AgNPs-cinnamon: Color light brown.

AgNPs-H1: Color yellow – spherical shape (1mL)

AgNPs-H3.5: Color red/orange – pentagonal shape (3.5mL)

AgNPs-H5: Color blue – prism shape (5mL)

AgNPs-H8: Color green – prism shape (8mL)

2. Preparation of sensidisks with control solutions, referred as targets systems. In that case were considered two blanks, one corresponding to the silver nitrate solutions and referred as Blank1 and another to the garlic or cinnamon extract, denoted by Blank2. The procedure followed consisted in:

Always working in a laminar hood, were cut filter paper discs with 1 cm of diameter and impregnated each one of them with 10 μ L of solutions. Then, in sterilized Petri dishes were placed each one of the impregnated discs that subsequently they were sealed. For each one of target systems were performed 3 repetitions.

3. Preparation of sensidisks with samples to be tested. For this case was prepared sensidisks, by the procedure mentioned before, for different concentrations of each one of the AgNPs prepared, that is:

- For AgNPs-Green suspensions were tested the concentrations 25%, 50%, 75%, and 100%.
- For AgNPs-Hydrazine suspensions were tested the concentrations of 20%, 60%, and 100%.

4. Preparation of Mueller Hinton Agar Cultivation Medium (MHB).

- Taking into account that the suggested concentration of the MHB in water is 38g/L, and that for each plate was required 20 mL of MHB, it was calculated the amount needed for, 25 for AgNPs-garlic and AgNPs-cinnamon.
- In a flask were poured 19 grams of Mueller Hinton agar in 500 mL of tri-distilled water and placed on the fire until it was boiled, for then be sterilized along with all the glassware to be used.
- In each plate were placed 20 mL of the agar solution in each plate.
- For Analysis performed to the samples of AgNPs-Hydrazine, the same procedure in the preparation of Mueller Hinton was realized.

5. Preparation of the inoculum.

- An isotonic solution 85.9% NaCl was poured in 4 test tubes.
- With help of a handle, a small amount of the different bacteria evaluated was taken from the direct colonies, and was carefully poured in the test tube containing the isotonic solution.

- Using a vortex to shake the test tubes were diluted the sample inside them until obtaining a turbidity comparable to 0.5 of McFarland, with the objective that each tube has approximately 105 UfC /mL.
6. Plate inoculation. For an optimal identification, the plates with agar (MHB) were labeled with the corresponding name of bacteria studied as well as with the code and concentration value of colloidal suspensions of AgNPs tested.
 - After maximum 15 minutes of inoculum preparation, was sowed the respective bacteria in each Petri dishes, previously prepared with agar.
 - With a swab was taken an amount of the inoculum and slide on the surface of the agar three times, rotating the plate 60° each time to cover the entire surface.
 - Finally, it was passed the swab through the peripheral part of the plate to be achieved a better uniformity in the sowing of the inoculum.
 7. Placement of sensidiscs on the respective plates, for which was required the use of the clamp, to press them gently on the agar to ensure that they are sufficiently impregnated on the surface. They should have been placed at a prudent distance, so that the halos did not overlap each other, and separated from the edge of the plate a minimal distance of 15 mm.
 8. Incubation, for which the plates were inverted so that the agar was in the upper part. Then, they were placed in a stove for 18 to 24 hours at 37°C. After the incubation time, the inhibition halos were removed and measured.

4.4.5 Determination of the Conductivity - Impedance of the polymer films prepared with AgNPs embedded.

For the determination of the conductivity of the thin films of the polymer prepared with PVA or Pectin, both with AgNPs embedded, the Electronic Impedance Spectroscopy technique (EIS) was used. This is a widely used and interesting electrochemical measurement method that is applied in many fields, such as electrochemistry, materials science, biology and medicine³¹. This technique is based on the use of an Alternating Current Signal that is applied to an electrode and determining the corresponding response.

In the most commonly used experimental procedure of EIS technique, a small potential signal (E) is applied to an electrode and its current intensity response (I) is measured at different frequencies. However, in certain circumstances, it is possible to apply a small current signal and measure the potential response of the system. The electronic equipment processes the potential-time ($E(\omega)$) and current-time ($I(\omega)$) measurements, resulting in a series of impedance values corresponding to each frequency studied. In general terms, the *Impedance* $Z(\omega)$ could be defined as an opposition measure, which presents a circuit to a current when a voltage is applied to a system, and it is calculated using Ohm's Law, and expressed in terms of amplitude, Z_0 , and a phase shift, ϕ .

$$Z(\omega) = E \cdot I \quad (\text{eq. 11})$$

The expression for $Z(\omega)$ is composed of a real part and an imaginary part. If the real part is plotted on the abscissa axis and the imaginary part is plotted on the ordinate axis of a graph, it is obtained a diagram called the Nyquist Diagram. As it is shown in the Figure 13 (left), each point in the Nyquist diagram represents the impedance value at a frequency³², and the information given by this diagram is obtained from the spectrum form.

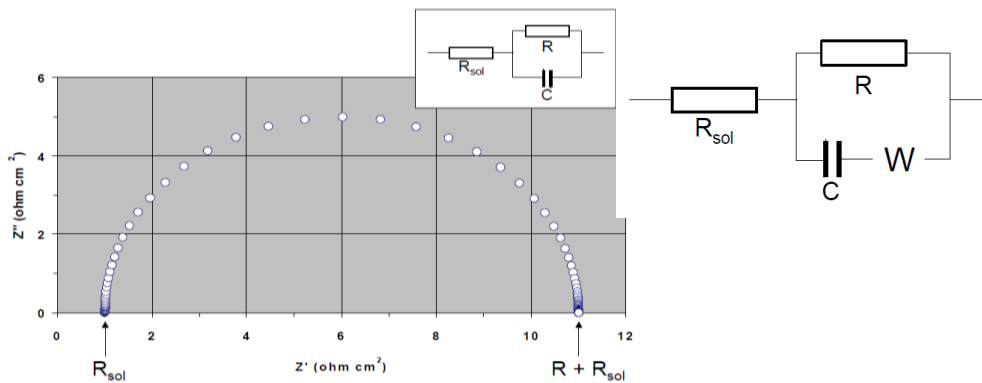


Figure 13 Nyquist Diagram (left) and its respective equivalent circuit (Randles circuit) (right)

Although the Nyquist diagram is the most used representation system, there is another diagram, called *Bode Diagram*, which is also obtained from an EIS analysis. In this diagram the logarithm of the impedance module ($\log |Z(\omega)|$) and the phase shift (ϕ) are plotted in function to the logarithm of the frequency ($\log(\omega)$) The information obtained from this type of representation is directed above all to the behavior as function of frequency.

The interpretation of an impedance spectrum requires the selection of a model that conforms to the experimental data; generally, it is done with electrical circuits whose

response is equivalent to the behavior of such data. This is a Randles Circuit, shown in the Figure 13 (right), which represents the “equivalent circuit”³³. For this research, the measurement of impedance was made in the Chemistry Laboratory of Yachay Tech University, and the schematic details of the experimental procedure developed it is shown in the Figure 14.

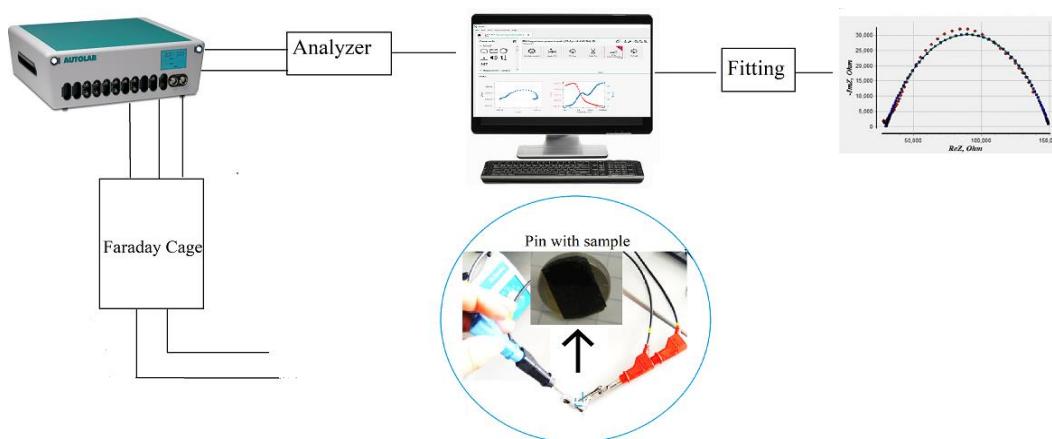


Figure 14 Scheme about Impedance measurements process.

The sample to be evaluated was supported on the electrode of conductive carbon, which was built using a SEM-pin made of aluminum, which was covered with conductive carbon adhesive, as is indicated in the inset of the Figure 14. All of the samples of films were adapted to the electrode dimensions, whose carbon adhesive was replaced in each measure, for the development of optimal measures.

For the appropriate analysis by EIS, it was required to take note of the area (A) and the thickness (t) of the thin film samples, for which a ruler and a micrometer screw were used. After the fitting of the data with Nyquist diagram, the *Resistance* value (ρ) was firstly obtained for each film sample, from which the resistivity values (R) can be calculated by the equation eq-C1, and subsequently the conductivity, by equation eq-C2, also can be determined.

$$R = \rho \frac{A}{t} \quad (\text{eq-C1}).$$

$$\sigma = \frac{1}{R} \quad (\text{eq C2}).$$

5. RESULTS, INTERPRETATION AND DISCUSSION

Chemical synthesis of AgNPs is presented in which their size is controlled by modulating of nucleation and particle growth processes, which is reached by means of suitable proportions used of reducing and capping agents, as well as the nature of them.

5.1. From Synthesis:

5.1.1. Chemical Synthesis:

In the Chemical Synthesis, a brown solution was obtained as a seed suspension, after placing the reducing and capping agents, a yellow to brown dispersion was obtained, which is considered the *Matrix Dispersion*, and a sample of that was taken for its analysis. When to this matrix dispersion was added 1 mL of AgNO_3 1 mM, a colloidal dispersion of yellow color was obtained. According to the volume of silver nitrate was added, the colors of the colloidal suspensions were changing, which was indicative of a change in the morphology of the nanoparticles. This change of color was due to that an increment in the silver nitrate volume leads to occurrence of the silver nanoparticles growth process¹⁸.

In the Figure 15 can be seen the different suspensions formed for each addition of AgNO_3 1mM. The suspension with the lowest amount of silver nitrate added corresponds to the yellow-like coloration, and the color was successively changing through of orange, pink, red, purple, violet, blue, turquoise, and green. In all of the cases could be evidenced a long stability, keeping their respective colors for several months. This range of colors allowed to establish a reference with which to compare the AgNPs suspensions obtained from the use of natural extracts³⁴.



Figure 15 Colloidal suspensions of AgNPs-Hydrazine (l-r) yellow-AgNPs-1H, orange AgNPs-2H, red AgNPs-3mL, purple AgNPs-H3.5, purple bluish AgNPs-H4, blue AgNPs-4.5, light blue AgNPs-5, greenish blue AgNPs-5.5, turquoise AgNPs-6, and green AgNPs-6.5.

The formation of a colloidal suspension was evidenced due to the distinction between solution and suspension, which became evident for the Tyndall effect³⁵. This effect is shown in Figure 16, in which the scattering of light can be seen when it passes through colloidal suspensions, an effect that is not seen in true solutions.

Colloidal particles are so small, in the order of nanometers that are not deposited; then the movement of the molecules is sufficient to keep them dispersed, which causes the light to not disperse when passing through the sample³⁵.



Figure 16 Tyndall effect scattering of AgNPs-H.

5.1.2 Combined Synthesis

When it is changed the reducing agent by the natural extracts, such as garlic and cinnamon extracts, were obtained AgNPs, which were evidenced by their appropriate characterization. However, the complete range of colors was not obtained using garlic extract or cinnamon extract, but the colors obtained for these AgNPs were limited only to a very small range, even when was added more and more nitrate silver to the mixture. The final color of these suspensions, shown in the Figure 17, were not reached immediately after forming the mixture, but it took certain time so that no further changes in color were observed. When was used garlic extract, the first addition of AgNO₃ solution 1 mM led to a yellow suspension, and adding the excess of nitrate of silver this turn to brown, without exhibiting appreciable changes in time, or after adding more silver nitrate or garlic extract.



Figure 17 Picture of combined synthesis of AgNPs with cinnamon bark extract as reducing agent.

5.1.3 Green Synthesis

In the Green Synthesis for obtaining AgNPs-garlic a soft yellow suspension was obtained, which after a few days (3-4 days) becomes brown as is shown in the Figure 18-(left), while for obtaining of AgNPs-cinnamon an orange suspension was obtained, Figure 18-(right). Both suspensions were characterized and the presence of AgNPs was evidenced.

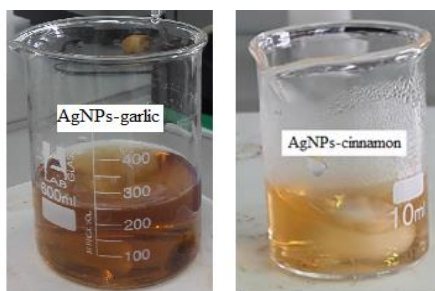
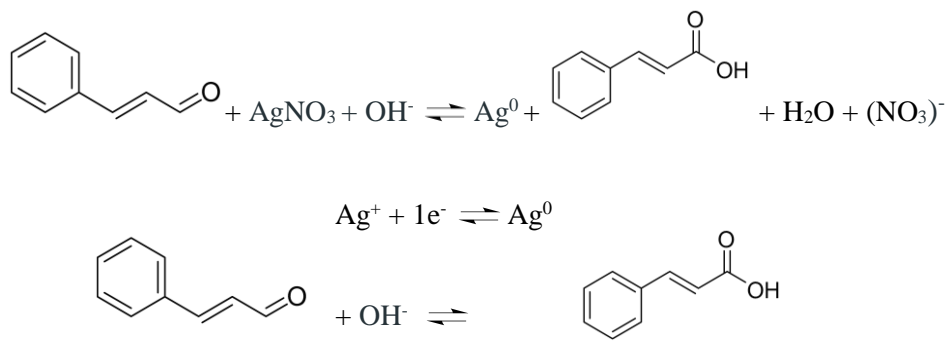
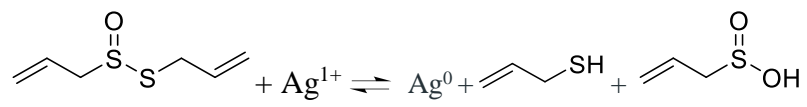


Figure 18 Picture of colloidal suspensions of AgNPs Green Synthesis.

As it was mentioned, the AgNPs formation by the coprecipitation method involved two principal processes; the nucleation and particles growth processes. These processes involved chemical reactions, specifically redox reactions, which have associated specific Standard Reduction Potential (E°)⁹, which are indicated in the Table 12. From the values of standard potential for each one of the redox reactions, it can be noted that they result in spontaneous reactions, with a positive voltage. In the different cases presented it is indicated as the reduction of silver, from a monovalent cation to metal atom, implies the oxidation of sodium borohydride to sodium borohydroxide for the formation of Seed Suspension.

In the case of the Chemical Synthesis, the silver reduction is accompanied of the oxidation of hydrazine, while in the Green Synthesis the reducing agent is the cinnamaldehyde whose oxidation leads to the cinnamic acid formation¹⁶. In the case of the allicin, the principal component of the garlic extract, is not a simple reaction and it is suspected that the silver reduction occurs through the oxygen of sulfoxide or the disulfide present in the structure of allicin³⁶.

Table 12 Redox reactions and standard potentials involved in the different method of synthesis of silver nanoparticles carried out⁹.

Redox Reactions	E° (V) ⁹
<p>Silver reduction with Sodium borohydride</p> $\text{AgNO}_3 (\text{aq}) + \text{NaBH}_4 (\text{aq}) \rightleftharpoons \text{Ag}^0 + \frac{1}{2} \text{H}_2 + \frac{1}{2} \text{B}_2\text{H}_6 + \text{NaNO}_3$ $\text{B}(\text{OH})_3 + 7\text{H}^+ + 8\text{e}^- \rightleftharpoons \text{BH}_4^- + 3\text{H}_2\text{O}$ $\text{Ag}^+ + 1\text{e}^- \rightleftharpoons \text{Ag}^0$	<p>-0.481</p> <p>0.80</p>
<p>Silver reduction with Hydrazine</p> $\text{N}_2\text{H}_4 + \text{AgNO}_3 \rightleftharpoons \text{Ag}^0 + \text{HNO}_3 + \text{N}_2$ $\text{N}_2 + 5\text{H}^+ + 4\text{e}^- \rightleftharpoons \text{N}_2\text{H}_5^+$ $\text{Ag}^+ + 1\text{e}^- \rightleftharpoons \text{Ag}^0$	<p>-0.23</p> <p>0.80</p>
<p>Silver reduction with Cinnamaldehyde</p>  $\text{Cinnamaldehyde} + \text{AgNO}_3 + \text{OH}^- \rightleftharpoons \text{Ag}^0 + \text{Cinnamic acid} + \text{H}_2\text{O} + (\text{NO}_3)^-$ $\text{Ag}^+ + 1\text{e}^- \rightleftharpoons \text{Ag}^0$ $\text{Cinnamaldehyde} + \text{OH}^- \rightleftharpoons \text{Cinnamic acid}$	<p>0.186</p> <p>0.80</p>
<p>Silver reduction with Aliicin</p>  $\text{Aliicin} + \text{Ag}^{1+} \rightleftharpoons \text{Ag}^0 + \text{S-allyl-L-cysteamine} + \text{S-allyl-L-cysteine sulfonic acid}$	<p>36</p>

5.2 Characterization of Silver Nanoparticles obtained.

5.2.1 FT-IR Spectroscopy to the analysis of AgNPs obtained by Green Synthesis.

In the Green Synthesis methods for the preparation of silver nanoparticles are involved the oxidation reaction of the principal component of the extracts, which act as reducing agents, and these happening reactions are not completely known. At the beginning it is required to confirm that the main component of extracts are the compounds suspected, the cinnamaldehyde for the case of cinnamon extract, and allicin for the case of garlic extract, in order to treat these compounds as the reducing agents involved in the synthesis process. By FT-IR spectroscopy it is possible confirms this, and also to evaluate the possible changes exhibited by the structure of these reducing agents after they participated in the formation of silver nanoparticles.

5.2.1.1 FTIR Spectroscopy of AgNPs-cinnamon

From the simple distillation of the cinnamon bark that was carried out to obtain its extract, a semi-transparent solution was obtained, a little dense, which was analyzed by FTIR spectroscopy to verify the presence of cinnamaldehyde, and corroborate that this molecule is the one that works as a reducing agent¹⁶.

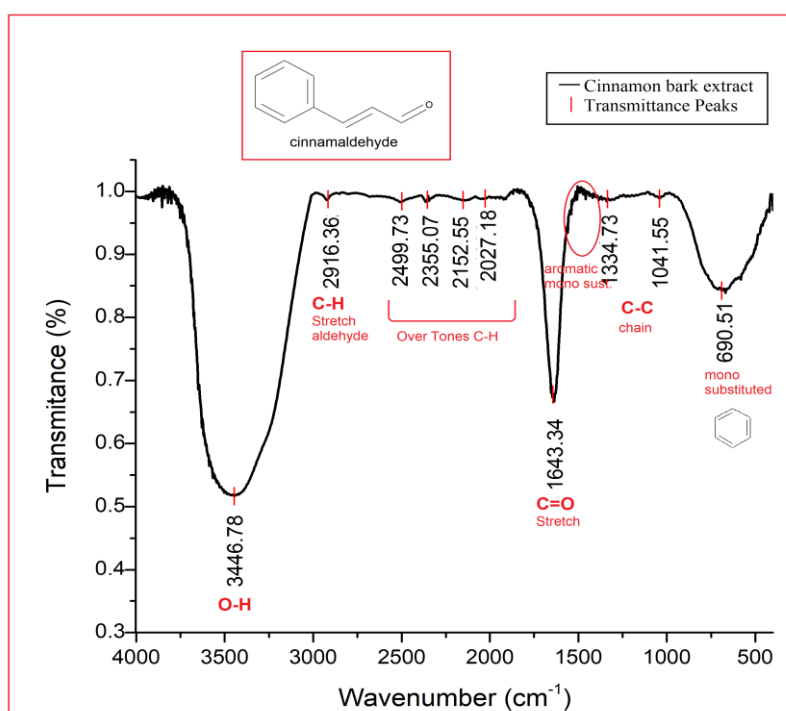


Figure 19 Spectrum obtained by FTIR spectroscopy for the extract of cinnamon bark.

The Figure 19 shows the FT-IR spectrum of the extract obtained from the cinnamon bark. In that it is possible to identify characteristic peaks for the cinnamaldehyde, such

as those appearing in: 690 cm^{-1} associated to the benzene, 1643 cm^{-1} to C=O stretch, 2916 cm^{-1} to C-H stretching characteristic for the aldehydes. Also it is observed a wide signal at 3446 cm^{-1} associated to the presence of O-H bond, which is evidence that it is an aqueous solution, and this wide peak is also responsible for the 2916 cm^{-1} peak not being prominent enough³⁷.

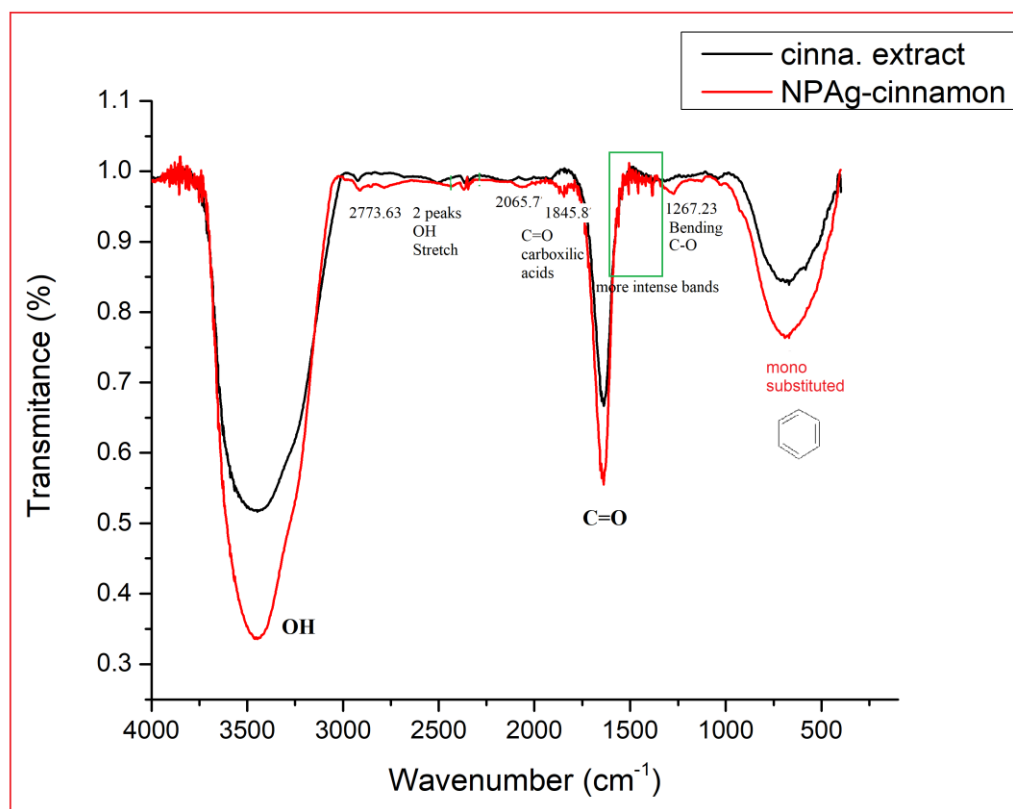


Figure 20 Spectrum FTIR obtained by spectroscopy of the resulting suspension of silver nanoparticles synthesized using cinnamon bark extract (AgNPs-cinnamon).

After the cinnamon extract is used in the synthesis of silver nanoparticles, the resulting colloidal suspension AgNPs-Cinnamon was analyzed by FT-IR spectroscopy, and the spectrum obtained is shown in the Figure 20. In this spectrum it is possible to note the slight changes with respect to the FTIR spectrum of the cinnamon extract alone. For example, the presence of a peak at 1845 cm^{-1} which is characteristic of C=O in carboxylic acids, and another in 1267 cm^{-1} that determines bending of C-O bond in a carboxylic acid³⁷. This proves that the cinnamaldehyde oxidation to cinnamic acid implies a little change in its structure, due to the silver atom attached to the acid. The other peaks are few modified.

5.2.1.2 FT-IR Spectroscopy of AgNPs-garlic

From the extraction of garlic with different types of solvents, alcohol extraction was chosen, since it is the best appearance. Approximately 50 mL of a yellow solution was obtained. To this yellow solution an FT-IR analysis was carried out to can know which the principal component of this solution is. The spectrum contain the principal peaks present in alliin molecule Figure 21.

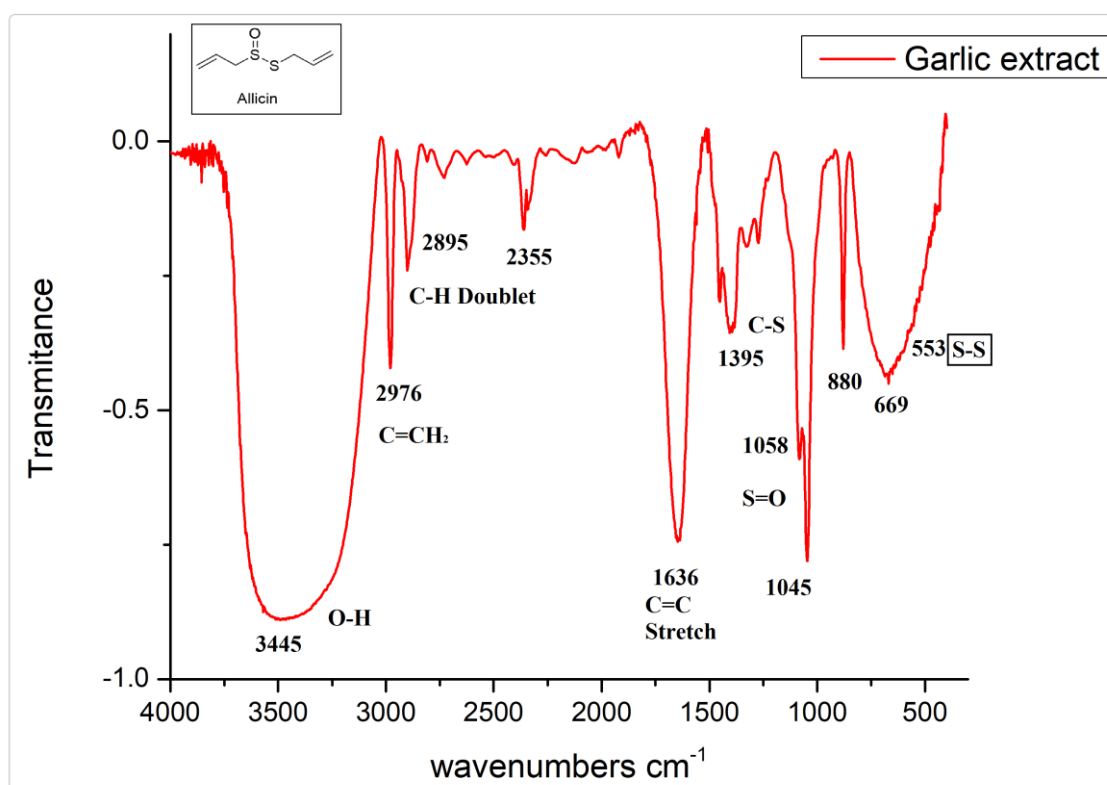


Figure 21 Spectrum obtained by FTIR spectroscopy for the extract of garlic.

In this spectrum the principal signals to analyze are: a weak peak between 500 cm^{-1} and 540 cm^{-1} ³⁷ associated to the S-S disulfide bond, which it is identified in the spectrum of the sample of AgNPs-garlic at 553 cm^{-1} , and is incorporated to peak at 669 cm^{-1} which represent to bending vibrations of $\text{C}=\text{CH}_2$. Other characteristic peak in the alliin molecule is the one that appears at 1058 cm^{-1} due to the S=O stretching vibrations, at 1395 cm^{-1} for C-S bond, and at 1636 cm^{-1} for C=C stretching vibrations³⁷. Therefore it is suggested that the major component in garlic extract is the alliin molecule.

Once the extract is used as a reducing agent in the synthesis of silver nanoparticles, the change of color exhibited by the solution could be indicative of a structural change of

the allicin. This fact is evidenced when the FT-IR spectrum of the resulting colloidal suspension of AgNPs-garlic is analyzed and shown in the Figure 22, in which is also shown the spectrum of garlic extract for comparison.

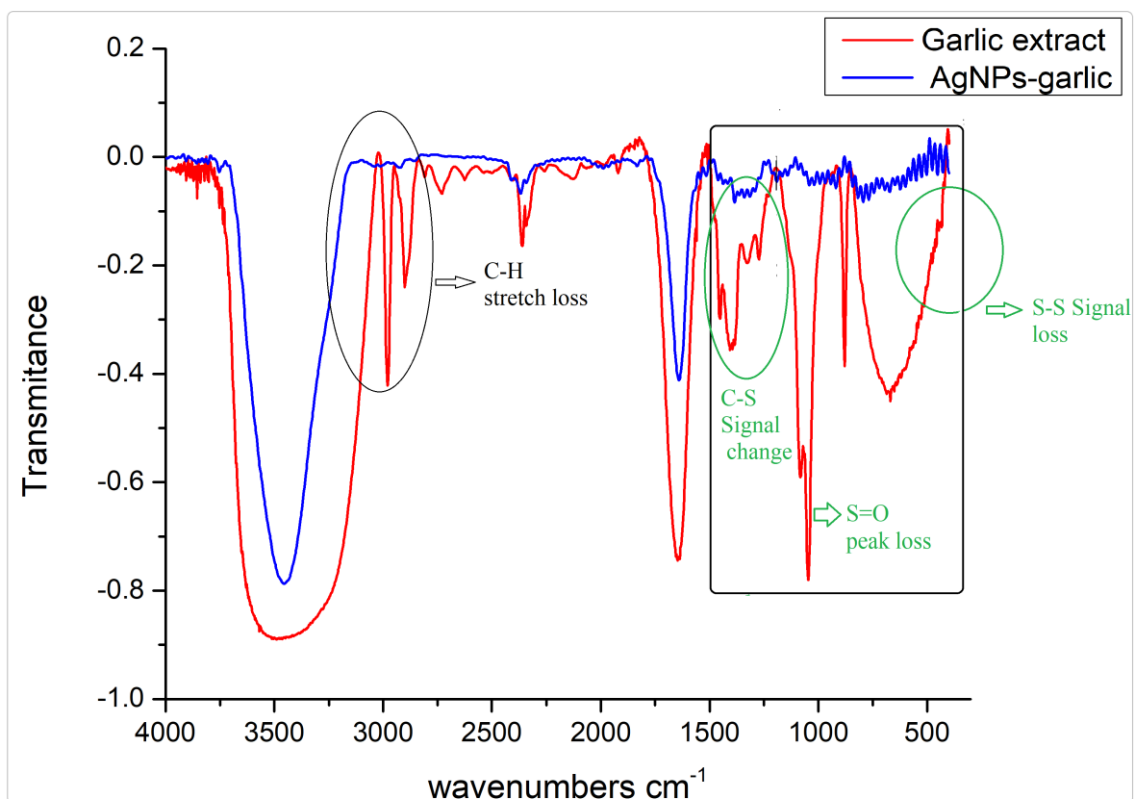


Figure 22 FTIR obtained by spectroscopy of the resulting suspension of silver nanoparticles synthesized using garlic extract (AgNPs-garlic).

In the FT-IR spectrum presented in the Figure 22 it is feasible to evidence the loss of some signals and changes in others when the AgNPs-garlic are formed. For example, the peaks associated with the S=O, S-S bonds disappear and the signal associated with C-S stretching vibration decreases, which suggest that the reaction is given through of the sulfoxide system³⁶, or for the breaking of disulfide bond.

5.2.2 Evaluation of Surface Plasmon Resonance using UV-VIS Spectroscopy

5.2.2.1 UV-VIS of AgNPs-Hydrazine

All colloidal suspensions of silver nanoparticles obtained from different methods showed absorption of light in the range of the visible spectrum. In Figure 23 it can see the different plasmonic bands (upper fig) corresponding to colloidal suspensions (lower fig) obtained using hydrazine as a reducing agent, in which it can be seen that the absorption wavelength range goes from 380 nm to 640 nm in measurements by UV-Vis spectroscopy. The maximum of the peak is changed to red as the volume of 1 mM AgNO₃ is progressively increased from 0 mL to 6.5 mL.

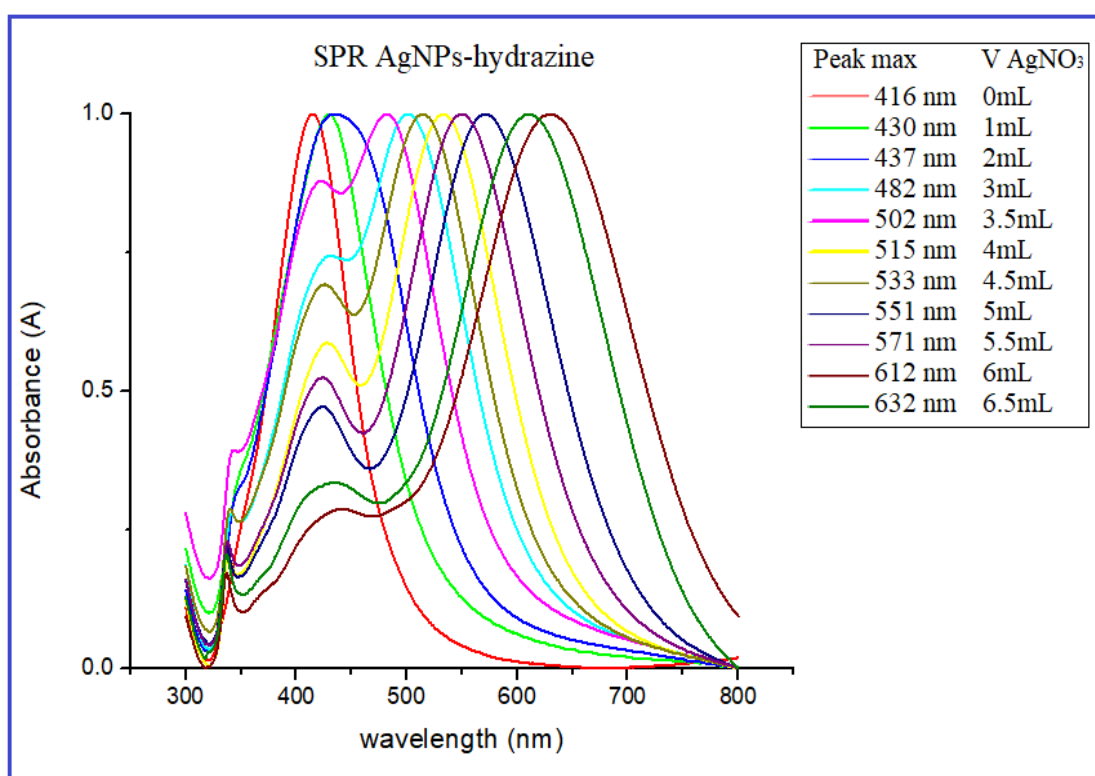


Figure 23 Spectra from UV-VIS spectroscopy of the SPR phenomenon of the different AgNPs-Hydrazine obtained using different volumes of silver nitrate 1 mM indicated in the inset of the figure.

From that figure it is feasible to observe that for the three first curves, corresponding to 0 mL, 1 mL and 2 mL of 1 mM of AgNO₃, only is evidenced one peak en 416 nm, 430 nm, and 437 nm, respectively. After that, it can be noticed the appearance of two more peaks, two of them around the 340 nm and 424 nm, and the main one that is shifted to red depending the volume of AgNO₃ added. For example, for the sample in which 3 mL of AgNO₃ was added the principal peak appear at 482 nm, while that for the sample with 6.5 mL of AgNO₃ the principal peak appear at 632 nm. The values of wavelength at which appear the more significant peaks are shown in the Table 13.

Volume of AgNO ₃ (mL)	0	1	2	3	3.5	4	4.5	5	5.5	6	6.5
Maximum peak (nm)	416	430	437	482	502	515	533	551	571	612	632
Second peak (nm)				424	432	426	428	425	424	436	444
Third peak (nm)				342	344	340	338	338	337	337	337

Table 13 Maximum Peaks with their wavelengths respective of the colloidal suspensions of the AgNPs-Hydrazine

The maximum absorption peak, called plasmatic band changes in the properties of nanoparticles such as size and shape, and the other 2 peaks appear by the interaction of 2 types of nanoparticles in samples that are of different size¹⁸.

The different colorations exhibited for the silver nanoparticles prepared using hydrazine are in concordance with the spectra obtained from UV-Vis spectroscopy^{38,39}. From the chromatic circle shown in the Figure 24 it is possible analyze the correspondence between the color exhibited by suspensions of nanoparticles and the main peak in their spectrum UV-Vis. As it is well known the reading of his chromatic circle imply that a solution orange has associate a wavelength around 430 nm, and so on³⁹.

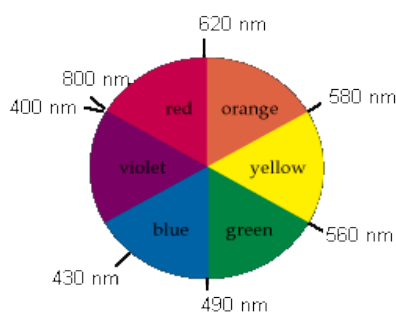


Figure 24 Chromatic Circle for the correspondence of color and wavelength.

5.2.2.2 UV-VIS Spectroscopy of AgNPs-combined

With respect to the synthesis of AgNPs using Natural Extracts as a reducing agent, the UV-Vis technique was performed in order to verify that the AgNPs have been formed, identifying signals of the plasmonic bands associated with the presence of nanoparticles. This analysis allows to identify the presence of nanoparticles and to evaluate the shift of plasmonic band comparable with those of the conventional Chemical Synthesis.

For the case of AgNPs-Combined (G), shown in Figure 25, it is feasible to observe the ability of the garlic extract to form nanoparticles, but no shift of the peaks occurs as the volume of AgNO_3 is increased, which is possibly due to the performance of the garlic extract as a good capping agent. In that case the main peaks appear in the region of wavelength around the 400 – 450 nm. Unfortunately, it was difficult to eliminate the initial decreasing exhibited in the spectrum of the Figure 25. It may be due to the aggregates of residual compounds from the synthesis, however, it can evidenced the presence of the plasmonic band around 450 nm.

The peaks in this graph are of less intensity than when hydrazine is used as a reducing agent, this may be happening because I have no control of the concentration of allicin that is acting as a reducing agent in AgNPs-Combined (G).

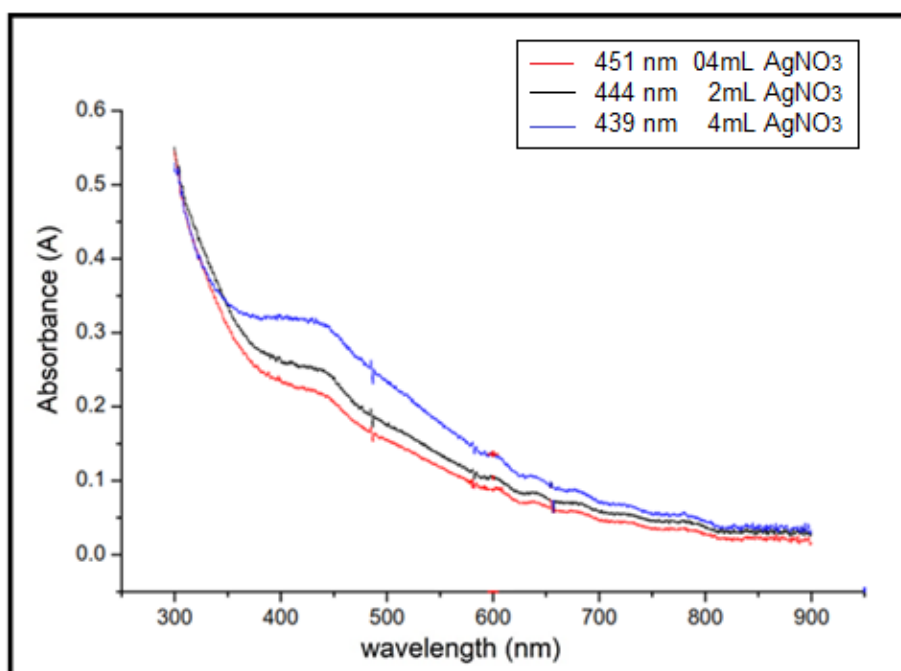


Figure 25 UV-VIS spectroscopy of the AgNPs-Combined(G) using garlic as reducing agent

Figure 26 shows the UV-Vis spectra of the AgNPs-Combined (C) where it can be seen the formation of AgNPs by the plasmonic bands around 450 nm¹⁸. Although it is also evident that the shift of plasmonic band, when adding volumes of silver nitrate, does not take place. Which suggests that AgNPs are not changing shape or size as is the case with chemical synthesis.

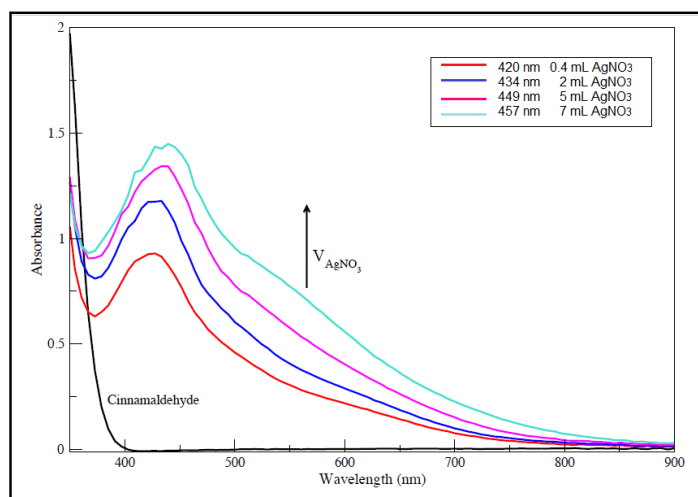


Figure 26 UV-VIS spectroscopy of the AgNPs-Combined (C) using cinnamon as reducing agent.

When the plasmonic band shift does not occur in the processes of Combined Synthesis, it can be inferred that the extracts used are in addition to reducing agents, good capping agents, this due to the molecules structures, (allicin and cinnamaldehyde), which are adhere in the NP and prevent them from changing^{40 41}.

5.2.2.3 UV-VIS spectroscopy of AgNPs-Green

When was carried out the Green Synthesis, from which were obtained AgNPs-garlic and AgNPs-cinnamon. For the case of AgNPs-garlic, shown in the Figure 27, two well distinguishable plasmonic bands appear, one of them at 480 nm and another one at 415 nm, this is because there are two different sizes of AgNPs formed. The first peak is due the more little NPs, and the second one is due to bigger NPs. The appearance of these two peaks and the width of the bands the width suggests a polydispersity in size of nanoparticles.

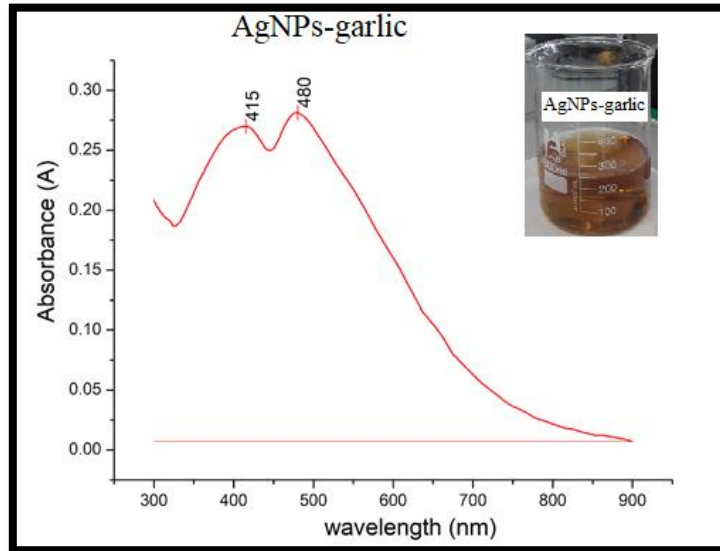


Figure 27 UV-VIS spectroscopy of the Green Synthesis of AgNPs-garlic

AgNPs-cinnamon

With respect to the AgNPs-cinnamon prepared, whose spectrum obtained by UV-Vis Spectroscopy is shown in the Figure 28, it is evidenced only one plasmonic band around 435 nm. This fact ensures the capacity of the cinnamon extract as and reducing and capping agent. It was no distinguished the peak at 415 nm appearing in the case of the nanoparticles obtained with garlic extract, and this can be the reason the different color exhibited for the colloidal suspension, shown in the inset of the Figure 28.

In this case only a single peak can be seen, which suggests a single size distribution of AgNPs.

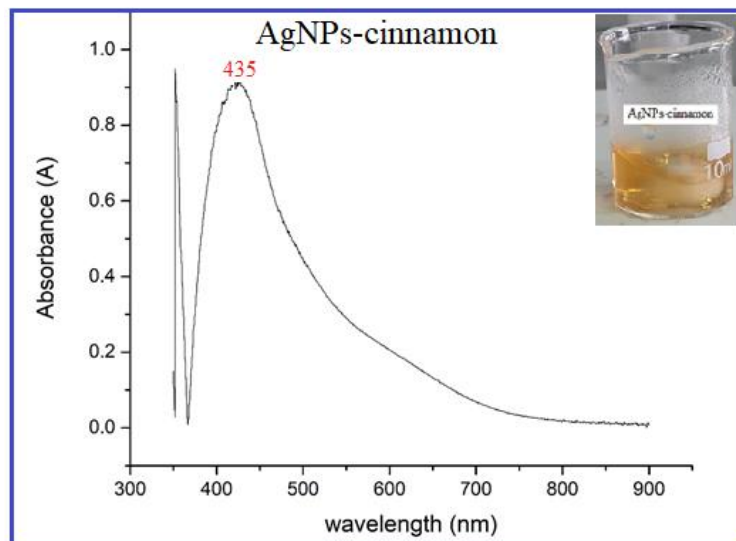


Figure 28 UV-VIS spectroscopy of AgNPs-cinnamon

5.2.3. Evaluation of the size and shape of silver nanostructures using Scanning Electron Microscopy.

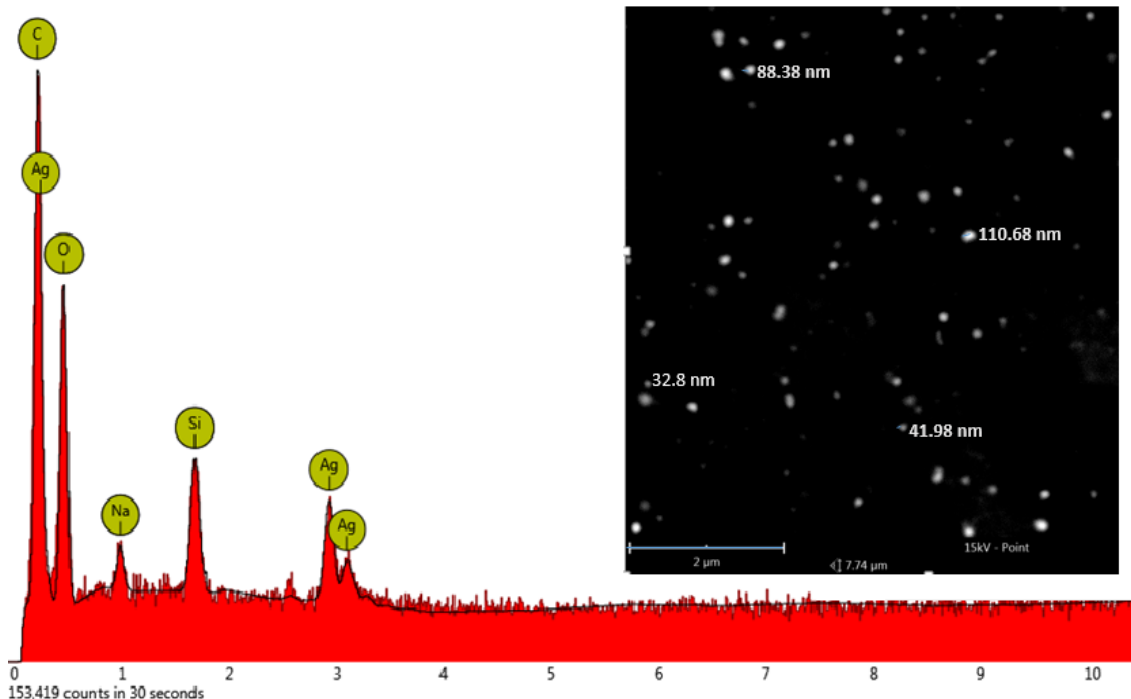


Figure 29 SEM of AgNPs-H6.5 with EDX-S information

For the analysis by Scanning Electron Microscopy (SEM) was possible to determine the presence of silver particles and to evidence that these particles have nanometric size, as is shown in Figure 29-Figure 31. For the case of nanoparticles obtained using hydrazine as reducing agent, in the Figure 29 it is shown one of the images obtained for them, specifically AgNPs-H6.5. In that figure it can be seen the nanoparticles, and it is indicated the size of some of them. An advantage of this technique is the possibility of obtaining elemental information because of the EDX-S analysis, shown in the Figure 29 in which it is evidenced the presence of long amounts of silver in the sample analyzed. Also it is evidenced the presence of other elements that were part of the synthesis process, such as sodium, oxygen, and carbon.

Scanning and Transmission Electron Microscopy

When to the scanning electron microscope it is adapted a detector of transmission, called STEM, the quality of images it is incremented, allowing a better visualization of size and shape of nanoparticles. The STEM analysis was performed in order to evidence the different shapes obtained in the Chemical and Green synthesis, to associate the kind of synthesis with the shape of nanoparticles obtained.

For nanoparticles obtained from Green Synthesis the analysis by STEM shows that both cinnamon bark and garlic extracts are good reducing agent, however, the morphology of the AgNPs-cinnamon corresponds to different shapes: spherical, cylindrical, and some prisms, as can be seen in the Figure 30 (upper panel), and the sizes of these nanoparticles are between 6 nm to 10 nm, however other sizes are obtained after some time of the synthesis, observing sizes around 60 nm and 80 nm.

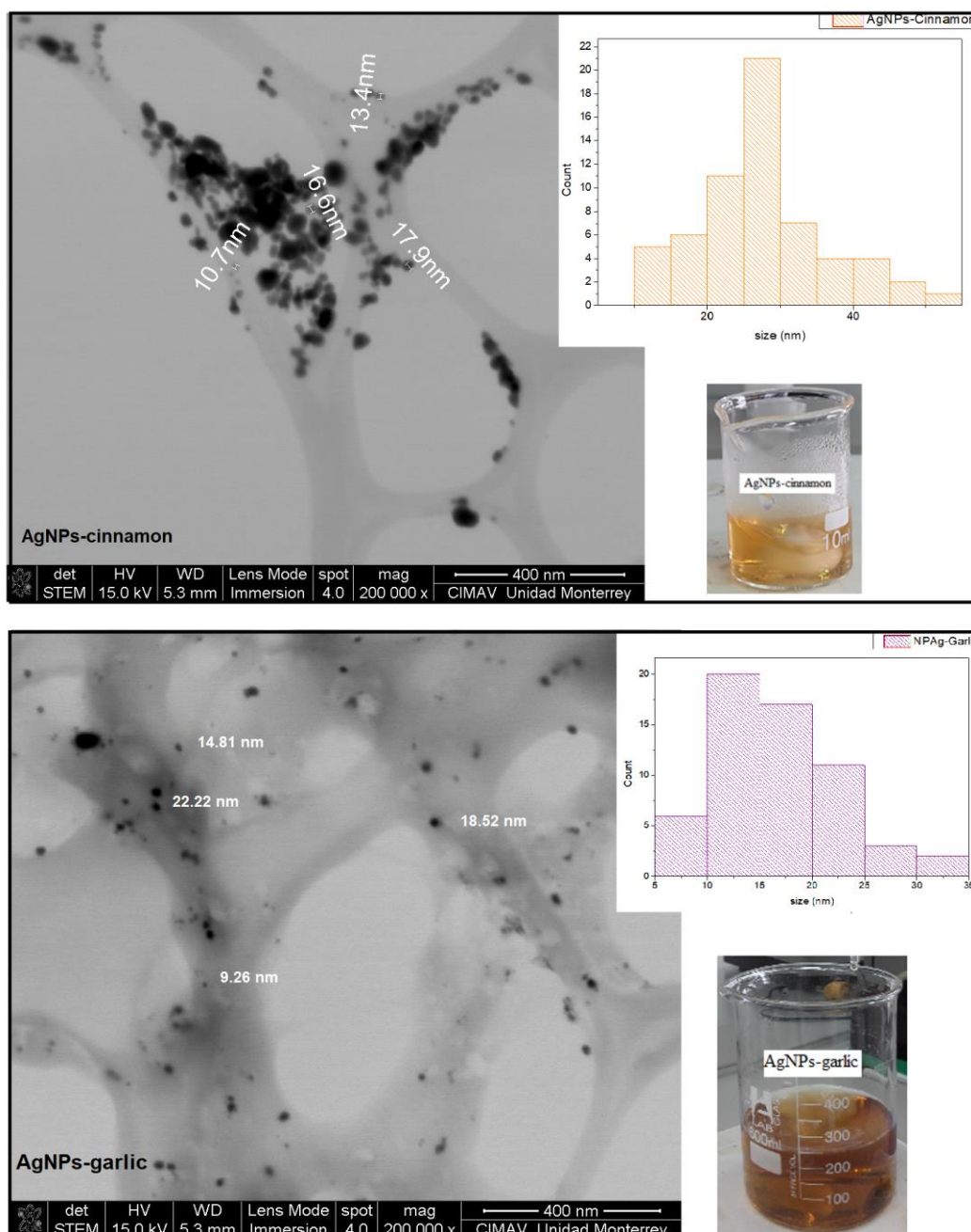


Figure 30 STEM images of (u) AgNPs-cinnamon (d) AgNPs-garlic, show the size and shape of the NPs.

The analysis by STEM for AgNPs-garlic is very useful for evidence that this natural extract is not only a good reducing agent, but overall an excellent capping agent because the shape of AgNPs is controlled, obtaining mainly spherical nanoparticles. The size of them ranged from 9 nm to 22 nm, as can be seen in the Figure 30(down panel). Although imperceptible to the eye the nanoparticles were shown to grow through other characterization techniques.

With respect to the nanoparticles obtained from Chemical Synthesis, whose images by STEM are shown in the Figure 31, it can be noted that the size and the shape of nanoparticles clearly depends on the amount of 1 mM AgNO₃ added. For example, in for the AgNPs-H3.5, for which were added 3.5 mL 1 mM AgNO₃, the images (a) and (b) indicate that the size oscillates between 9 nm to 12 nm, presenting a spherical shape. As the volume of AgNO₃ is increased, as for the case of AgNPs-H5 shown in figures (c) and (d), their shape changed because the spheres begin to faceted by a growth process or the aggregation of little particles, and also their size increased.

Finally, the last case presented in the Figure 31, for an added volume of 1 mM AgNO₃ of 8 mL, the images for AgNPs-H8 shown in figures (e) and (f), confirm that their size can reach values as big as 56.52 nm, and evidencing the presence of the perfect nanoprisms, an interesting shape for this nanoparticles. When forming nanoparticles by chemical synthesis, it starts with a seed suspension with AgNPs that have a spherical morphology thanks to the effect of citrate as a capping agent⁴¹, then in the growth process when adding AgNO₃ the spherical particles are added to each other making these spheres pointed shapes, until polyhedra such as octahedra, cubes or bipyramides⁴¹ are formed until they reach more stable forms such as triangular plates, or nanoprisms⁴².

The results from STEM technique represent an evidence of that in the method of Chemical Synthesis is feasible have control of the size and shape of the silver nanoparticles prepared, controlling the dependence of the size of nanoparticles on the added volume of 1 mM AgNO₃.

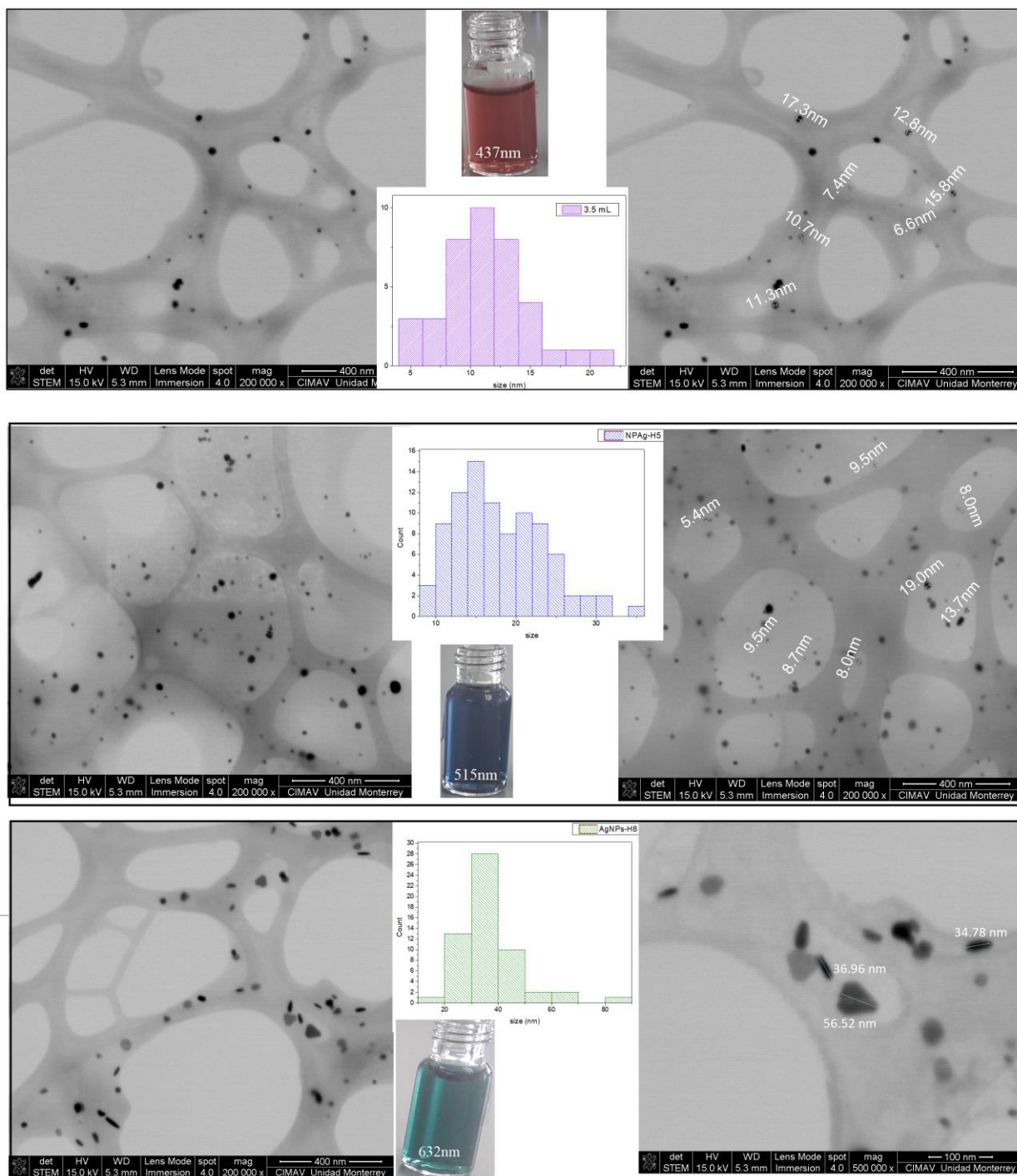


Figure 31 STEM images a) spherical shape of AgNPs-H3.5, b) size of AgNPs-H3.5, c) shape of AgNPs-H5, d) size of AgNPs-H5, e) prism shape of AgNPs-H8 and f) size of AgNPs-H8.

5.2.4. Evaluation by Dynamic Light Scattering (DLS) and by Z-potential of silver nanoparticles obtained.

5.2.4.1 DLS of AgNPs obtained by the Green Synthesis.

The analysis of DLS results in a graph of different diameter of the obtained system with their respective intensities. This graph is shown in the Figure 32 for the case of the AgNPs-cinnamon, and in it is possible to identify three peaks with different intensity percentages. Each one of them corresponds to three different sizes of silver nanoparticles identified in the sample, which range from 2.94 nm to 66.41 nm. However, the value by Z-Average for the nanoparticles size suggests a particle diameter of 115.4 nm, being very different to those before mentioned. The reason of that can be attributed to the possible different shapes formed during the synthesis process, which is not considered by this analysis, since that it assumes a spherical shape for the nanoparticles. In fact, the message given for the “Result quality”, presented in the Figure 31 suggests problems with the calculation of the average size.

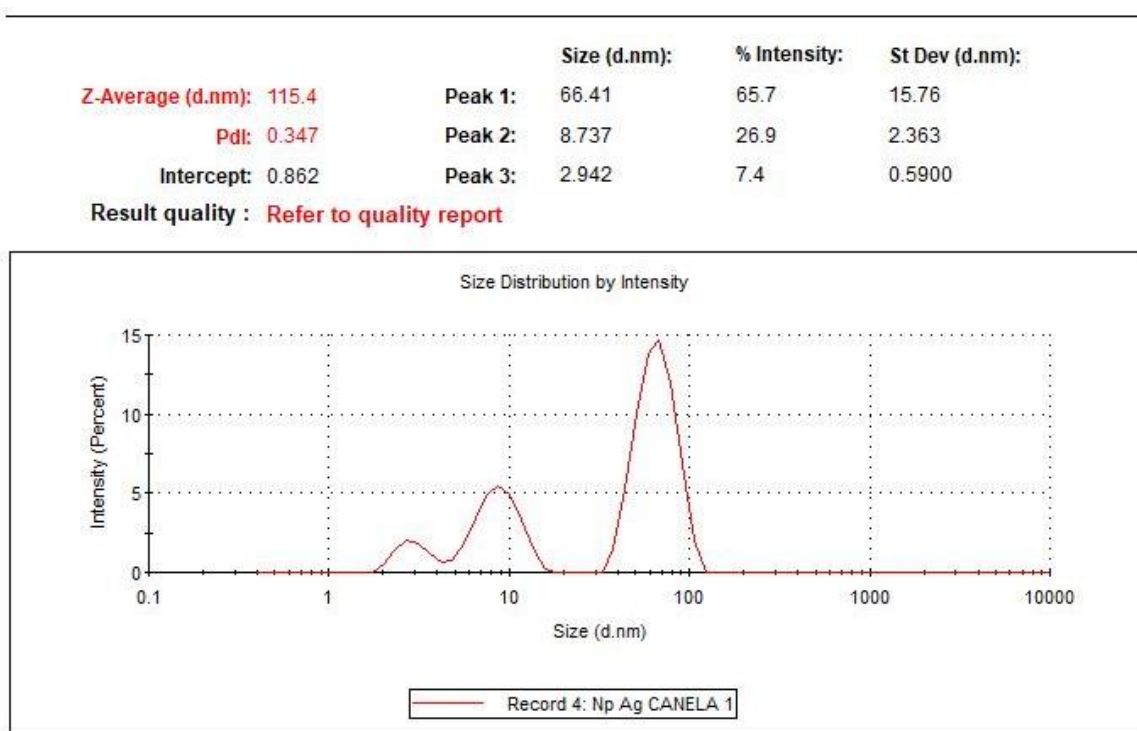


Figure 32 Distribution of sizes evaluated by DLS for AgNPs-cinnamon.

With the Z-potential analysis it can be evaluated the potential associated to the surface of nanoparticle, as well as also give information about the stability of the nanoparticles for values of Z-potential ranged from -30 mV to 30 mV. The results obtained from this

analysis are shown in the Figure 33, from which it is feasible to see that the AgNPs-cinnamon have a surface charge, which has associates a surface electric potential, that is the Z-potential, of -13.6 mV. This value of surface electric potential suggests that the AgNPs-cinnamon present a certain stability, which had been suspected by the time these systems remained apparently unchanged.

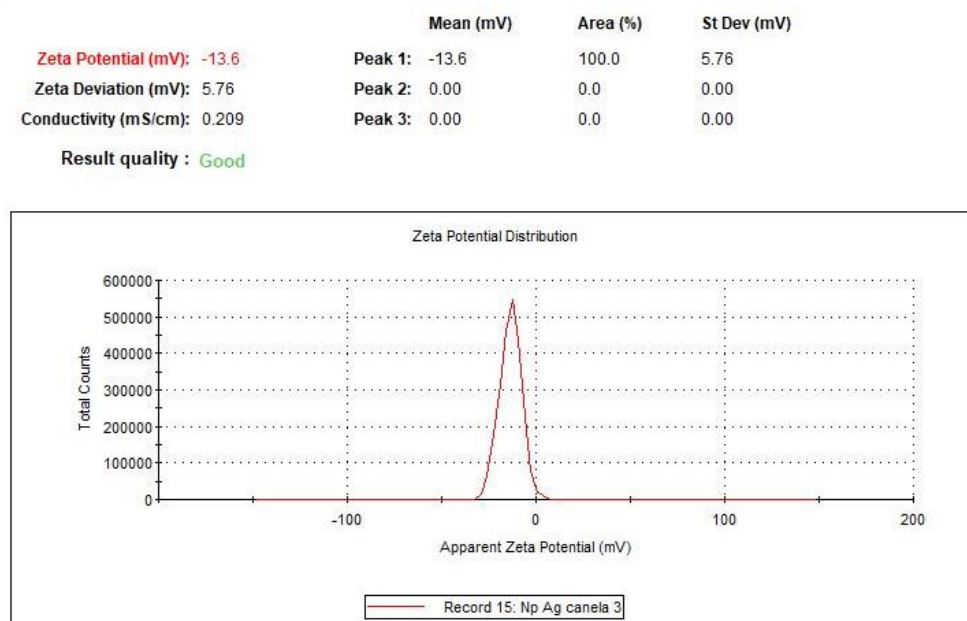


Figure 33 Zeta potential of AgNPs-cinnamon.

With respect to the silver nanoparticles obtained from garlic extract as the reducing agent, its evaluation by DLS it is shown in the Figure 34. By this analysis is evidenced the lower polydispersity with respect the size presented in this system, AgNPs-garlic, compared with the previous system described. Only one peak is identified, corresponding to the average value of particles diameter of 216 nm. It can be seen in the report that the “Result quality” is Good. In spite of it bigger average size, compared with AgNPs-cinnamon, the shape of the AgNPs-garlic remains spherical. Therefore, it is evidenced the good ability of the allicin to control the nanoparticle shape during the grow process. For ensure this suggestion, it is necessary to carry out anew analyzes by controlling the time of sounding, and even to increase the quantity of stabilizing agent to avoid agglomerations by aggregation of little structures, however this experimental procedure were not performance.

AgNPs-garlic

	Size (d.nm):	% Intensity:	St Dev (d.nm):
Z-Average (d.nm): 216.0	Peak 1: 216.7	100.0	62.58
Pdl: 0.232	Peak 2: 0.000	0.0	0.000
Intercept: 0.907	Peak 3: 0.000	0.0	0.000
Result quality : Good			

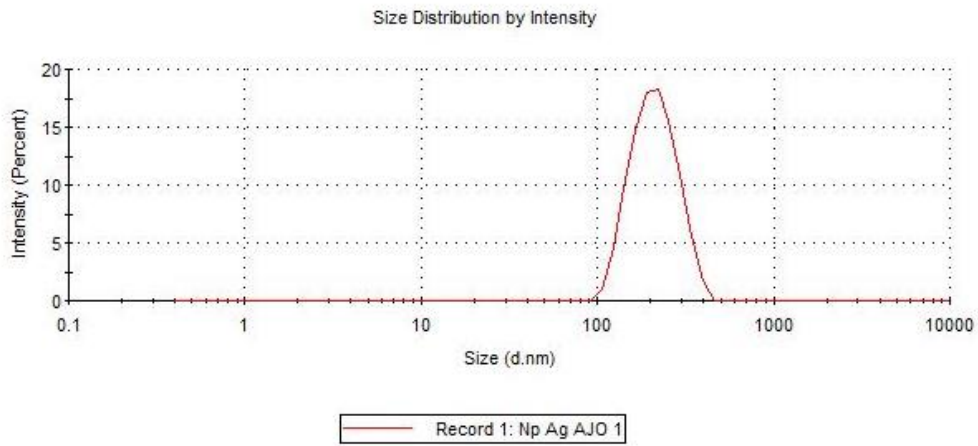


Figure 34 Distribution of sizes of AgNPs-garlic obtained from DLS

	Mean (mV)	Area (%)	St Dev (mV)
Zeta Potential (mV): -11.8	Peak 1: -11.8	100.0	4.32
Zeta Deviation (mV): 4.32	Peak 2: 0.00	0.0	0.00
Conductivity (mS/cm): 0.149	Peak 3: 0.00	0.0	0.00
Result quality : Good			

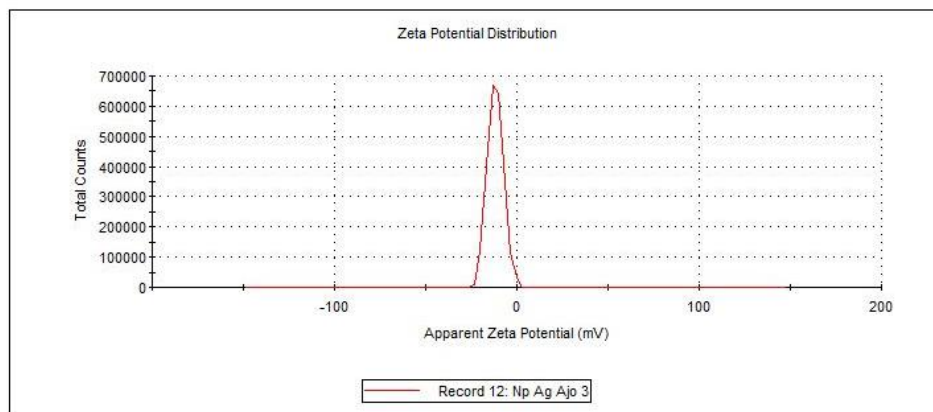


Figure 35 Z-potential of AgNPs-garlic.

In the Figure 35 it is shown the results of Z-potential of AgNPs-garlic, it can be seen a unique peak at -11.8 mV which represents the surface electric potential, giving information about the electrical stability of the AgNPs-garlic.

5.2.4.2 DLS of AgNPs-Hydrazine

Table 14 Size-Average and Z-potential of samples of AgNPs-Hydrazine

Sample	Size-Average (nm)	Peak 1 (%)	Peak 2 (%)	Z-Potential (%)
3.7 mL red	62.00	69.21	8.039	-19.2
5 mL blue	84.09	110.9	16.1	-18.4
8 mL green	30.20	78.69	6.37	-13.7

The data shown in Table 14 are Size-Average and Z-Potential corresponding to the samples of AgNPs-Hydrazine, which allow to probe the stability of the nanoparticles formed from different added volumes of 1 mM AgNO₃, according to the values of Z-potential obtained, which are minors that -20 mV. The surface electric potential associated at these nanoparticles also allows have evidence that the AgNPs-Hydrazine have surface charges similar. In the Table 14 also is can be seen different peaks for the size of particle. It is in concordance with the UV-vis spectroscopy Figure 23 which give two or three peaks which shown different size of AgNPs-Hydrazine, and also are evidenced in STEM analysis Figure 31.

5.3 For the applications:

5.3.1 Electrochemical Impedance Analysis of the polymers with AgNPs

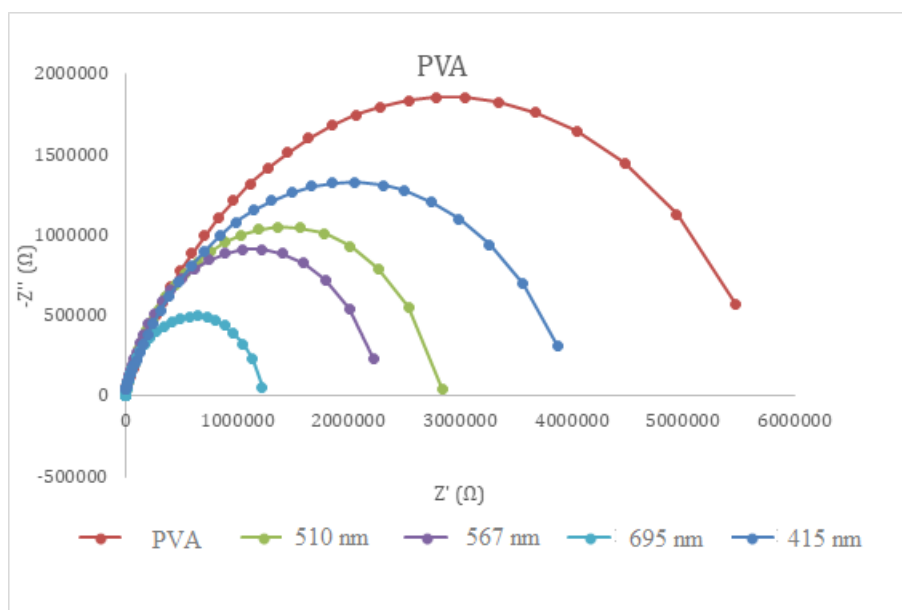


Figure 36 Nyquist plot. Electrochemical Impedance of thin films of PVA with AgNPs-Hydrazine.

The Figure 36 indicates the impedance values of the 5 thin films formed with PVA and AgNPs-Hydrazine, and it is observed that the sample with the bigger value of impedance is that was made only with PVA, and a decrease of it is observed when AgNPs are added. The lower value corresponds to film with the AgNPs of major size, those that present the Surface Plasmon Resonance at approximately to a wavelength of 695 nm. Then, with values taken of area and thickness of the film, the resistivity and the resistance were obtained by this analysis, and from them the conductivity of the films was calculated using the equations eq I1 and eq I2. The results are showed in Table 15, and from them it is feasible probate that the AgNPs contribute to the conductivity of the film prepared from PVA polymer. The conductivity value for PVA has a magnitude order of 10^{-11} S/m, which is comparable with the values reported in literature⁴³.

For the film PVA-based with AgNPs embed, the values of conductivity have a magnitude order of 10^{-10} S/m, which completely evidence the increase in the conductivity for films. There is a proportional relationship between the conductivity and the size of AgNPs embedded, that is, the larger the nanoparticles the larger the conductivity. It can be attributed to the presence of more ions and electrons going through of all system.

Table 15 Conductivity calculated with data obtained in the impedance study for thin films of PVA with AgNPs-Hydrazine

	R_p [MΩ]	A [mm²]	t [mm] x 10⁻³	R [Ωm] x 10⁹	σ [S/m]
PVA	5.94	104	0.0117	10.4	9.59×10^{-11}
415 nm	5.15	104	0.0708	7.56	1.32×10^{-10}
v 510 nm	4.31	104	0.119	3.83	2.61×10^{-10}
567 nm	2.86	104	0.079	3.87	2.66×10^{-10}
695 nm	2.31	104	0.062	3.77	2.58×10^{-10}

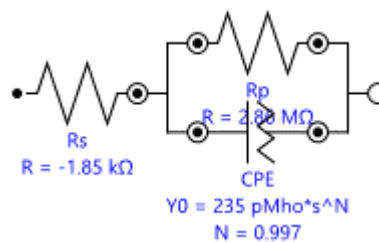


Figure 37 Equivalent circuit (Randles circuit) for polymer PVA AgNPs-695nm

Figure 36 shows the circuit equivalent to the Impedance data taken for the PVA thin film sample AgNPs-695 nm, it is a Randles type circuit that represents a single

semicircle, with a capacitor and a resistor, the first it represents one unit of time, and the second one represents the resistance of the system.

5.3.2 Antibacterial Analysis of the AgNPs-Green.

The results obtained from the bactericidal analysis are shown in the Table 16 and Table 17 for the case of AgNPs-garlic and AgNPs-cinnamon, respectively.

Table 16 Halos of inhibition for four bacteria tested with AgNPs-garlic at five different concentrations. The results correspond to the average for three repetitions for each sample.

AgNPs-garlic				
BACTERIA	C7230 (E.coli)	PE52 (Pseudomona)	AN54 (Acinetobacter haemolyticus)	29213 (Staphylococcus aureus)
	Halos (mm)			
SAMPLE				
Blank1: Silver Nitrate	10	11	10	9
Blank2: Garlic extracts	6	6	6	6
AgNPs 25%	6	6	6	6
AgNPs 50%	7	6	6	6
AgNPs 75%	7	10	6	6
AgNPs 100%	7	10	6	6
AgNPs 250%	7	8	6	6

From the results shown in Table 16, it can appreciate that when the Blank1 analysis was carried out, 10-mm inhibition halos were observed, which verified the anti-bacterial effects of cationic silver. On the other hand, the Blank2 and the AgNPs-garlic solutions gave halos of 6 and 7 mm, which are not significant (6 mm measured disk).

Samples were evaluated at different concentration of nanoparticles prepared from the initial sample, this last denoted as AgNPs-garlic 100%. It can be noted a slight increase of the effectiveness of the bactericidal activity when is incremented the concentration, however, for the more concentrate sample AgNPs-garlic 250%, which is prepared by reducing the volume of the solvent, did not present a significant increment of inhibition halos. In the Figure 37 it can be seen some samples under evaluation.

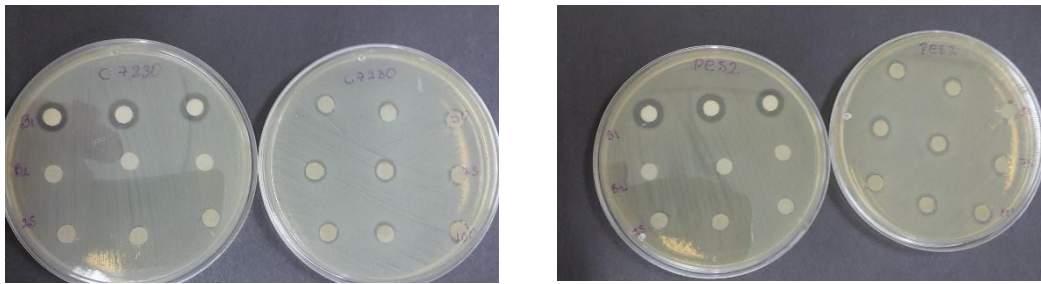


Figure 38 Antibacterial study of NPs-Ag garlic analyzed with C7230 E.coli, PE53 pseudomone.

For the case of the bactericidal activity evaluation of AgNPs-cinnamon, whose results are shown in t

he Table 16, it can be observed that for the Blank1 again gave halos of inhibition corresponding to the cationic silver, when working with the AgNPs-cinnamon in low concentrations no considerable halos were observed, however when the concentration was increased to 75% and 100%, shown in the Figure 39, larger diameter halos were obtained for C7230 and PE52, being of 9 mm and 10 mm, respectively. Then suspensions of AgNPs-cinnamon then these were concentrated in 5 and 10 times more named as 500% and 1000% to analyze if it increases the inhibition of bacterial growth, obtaining in this case larger diameter of halos de inhibition, for example, for 500% halos of inhibition up to 15 mm in diameter for PE52, 14 mm for AN54, 12 mm for C7230 and 10 mm for 29213. For the sample corresponding to AgNPs-cinnamon 1000% these values are approximately preserved, that is to say there is no increase of inhibition.

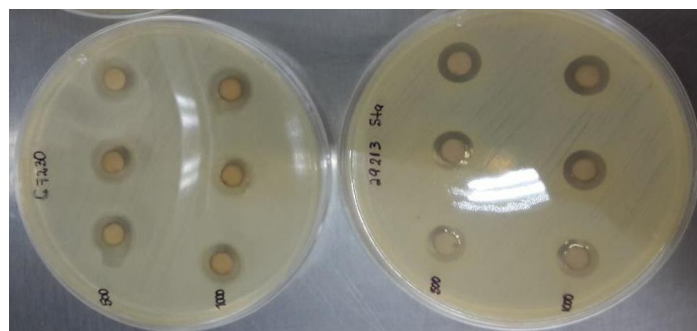


Figure 39 : Antibacterial study of NPAg-cinnamon increasing the concentration 500%, 1000% Analyzed with C7230 E.coli, and 29213 Staphylococcus

Table 17 Halos of inhibition for four bacteria tested with AgNPs-cinnamon at six different concentrations. The results correspond to the average for three repetitions for each sample.

AgNPs-cinnamon				
BACTERIA	C7230 (E.coli)	PE52 (Pseudomona)	AN54 (Acinetobacter haemolyticus)	29213 (Staphylococcus aureus)
	Halos (mm)			
Blank1: Silver Nitrate	10	11	10	7.67
Blank2: cinnamon extracts	6	6	6	6
AgNPs 25%	6	6	6	6
AgNPs 50%	7	9	6	6
AgNPs 75%	9	10	7	6
AgNPs 100%	9	10	7	7
AgNPs 500%	12	14.33	14	10
AgNPs 1000%	11	15.33	14	10

These high concentrations of colloidal suspensions were analyzed by UV-VIS in the laboratories of Yachay Tech University in Ecuador, to ensure that the characteristic plasmonic bands of AgNPs-cinnamon can be identified, and, it can be seen in the Figure 40 (l)Figure 40. This evaluation showed an absorbance peak at approximately 300 nm, although the expected value corresponds to the region of 400 nm.

The peak at 300 nm, and no at ~400 nm, it indicate that there is no reduction in silver, therefore the characteristic peak of silver nanoparticles of 380 to 400 nm⁴⁴ not be being looked at. What be observed is the peak of silver nitrate that occurs at approximately 300 nm Figure 40(r). However the inhibition halos of all of the samples, those with greater concentration, such as AgNPs-cinnamon 5 and 10 times more centered have higher halo of inhibition, this phenomenon will be studied with other methods posteriorly.

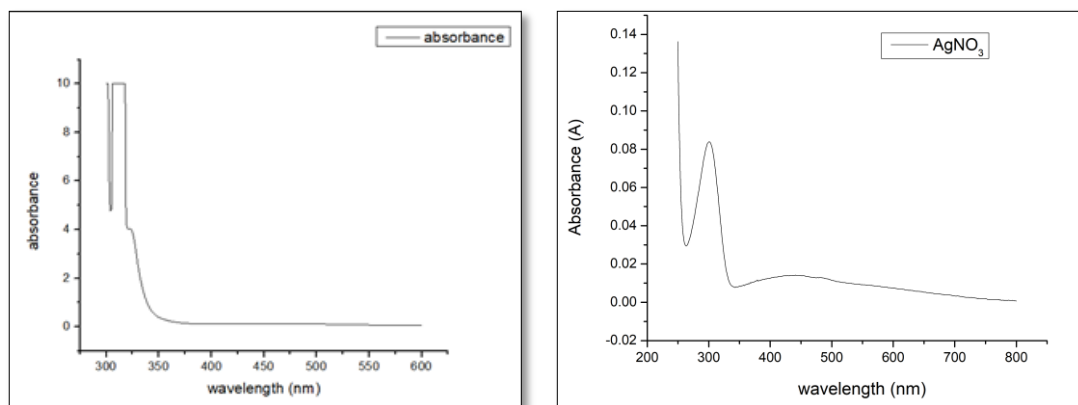


Figure 40 UV-VIS AgNPs-cinnamon 500% (l) UV-Vis AgNO₃ (r)

Finally, the bactericidal activity study of the AgNPs-Hydrazine was carried out, in which it was observed that the silver nitrate being present in lower concentrations, so that it is comparable with the amount added in the different colloidal suspensions of AgNPs, in certain cases present halos of inhibition of smaller diameter. On the other hand, it is observed that the AgNPs-Hydrazine do not present halos of inhibition of importance in any case, as it can be seen in the Table 18, Table 19, Table 20 and Table 21.

Table 18 Halos of inhibition for four bacteria with NPs-Ag-HI, at three different concentrations. The results correspond to the average for three repetitions for each sample.

AgNPs-HI				
BACTERIA	DH5α (E.coli)	PAO1 (Pseudomona)	AN2 (Acinetobacte)	29213 (Staphylococcus aureus)
	Halos (mm)			
Blank1: Silver Nitrate	8	9	8	7
Blank2: Control Solution 25%	6	6	6	6
AgNPs 20%	6	6	6	6
AgNPs 60%	6	6	6	6
AgNPs 100%	6	6	6	6

Table 19 Halos of inhibition for four bacteria with NPs-Ag-H2, at three different concentrations. The results correspond to the average for three repetitions for each sample.

AgNPs-H2

BACTERIA SAMPLE	DH5α (E.coli)	PAO1 (Pseudomona)	AN2 (Acinetobacte)	29213 (Staphylococcus aureus)
	Halos (mm)			
Blank1: Silver Nitrate	9	9		7
Blank2: Control Solution 50%	6	6	6	6
AgNPs 20%	6	6	6	6
AgNPs 60%	6	6	6	6
AgNPs 100%	6	6	6	6

Table 20 Halos of inhibition for four bacteria with NPs-Ag-H3, at three different concentrations. The results correspond to the average for three repetitions for each sample.

AgNPs-H3

BACTERIA SAMPLE	DH5α (E.coli)	PAO1 (Pseudomona)	AN2 (Acinetobacte)	29213 (Staphylococcus aureus)
	Halos (mm)			
Blank1: Silver Nitrate	6	8	6	8
Blank2: Control Solution 75%	6	6	6	6
AgNPs 20%	6	6	6	6
AgNPs 60%	6	6	6	6
AgNPs 100%	6	6	6	6

Table 21 Halos of inhibition for four bacteria with NPs-Ag-H4, at three different concentrations. The results correspond to the average for three repetitions for each sample.

AgNPs-H4

BACTERIA \ SAMPLE	DH5α (E.coli)	PAO1 (Pseudomona)	AN2 (Acinetobacte)	29213 (Staphylococcus aureus)
	Halos (mm)			
Blank1: Silver Nitrate	9	10	7	9
Blank2: Control Solution 100%	6	6	6	6
AgNPs 20%	6	6	6	6
AgNPs 60%	7	7		6
AgNPs 100%	8	8	6	6

The Figure 41 shown a sample of the dishes Petri corresponding to the analysis carried out for evaluate the bactericidal activity of the AgNPs-H4 with the bacteria identified as DH5α. It can be seen the low activity.



Figure 41 Antibacterial study of AgNPs-H4, analysis with DH5α.

6. CONCLUSIONS AND RECOMMENDATIONS.

1. By the Green Synthesis it is feasible to check the reducing effect of garlic and cinnamon bark extracts for the synthesis of silver nanoparticles, being the principal actors in this reduction process the allicin in AgNPs-garlic, and cinnamaldehyde in AgNPs-cinnamon, which were evidenced by FT-IR analysis.
2. With the Combined Chemical-Green Method it was possible to determine that the extracts are excellent capping agents for the synthesis of silver nanoparticles.
3. By modulating the nucleation and growth processes in the synthesis of silver nanoparticles the size and shape of the nanoparticles can be controlled, obtaining as result that the smaller ones are spherical, and the larger ones are nano-prisms.
4. Impedance analysis indicates that the conductivity of a non-conductive polymer, such as PVA, can be increased by placing with AgNPs.
5. The Kirby Bauer analysis for the study of the antibacterial activity of the silver nanoparticles gave partially successful results, however, the method of analysis can be improved.

For all the above in this work it is concluded that the synthesis system developed with the natural extracts of garlic and cinnamon bark are very efficient since, they allowed to synthesize silver nanoparticles with controlled particle size and shape, and with applications as conductive materials and with potential bactericidal activity.

This work could be improved by optimizing the extraction and characterization methods of the extract of garlic and cinnamon extract, because the values of yield and purity were not analyzed.

7. BIBLIOGRAPHY

- (1) Applications, P. F. Food Nanotechnology. *Inst. Food Technol.* 1003, 23–25.
- (2) Peterson, C. L. Nanotechnology : *IEEE Technol. Soc. Mag.* **2004**, 23, 9–15.
<https://doi.org/10.1109/MTAS.2004.1371633>.
- (3) Monge, M. Investigación Química Nanopartículas de Plata : Métodos de Síntesis En Disolución Y Propiedades Bactericidas. **2009**, 33–41.
- (4) Complutense, R.; Veterinarias, C. NANOPARTÍCULAS DE PLATA: APLICACIONES Y RIESGOS TÓXICOS PARA LA SALUD HUMANA Y EL MEDIO AMBIENTE. **2013**, 7 (2), 1–23.
- (5) Ip, M.; Lui, S. L.; Poon, V. K. M.; Lung, I.; Burd, A. Antimicrobial Activities of Silver Dressings : An in Vitro Comparison. **2006**, 59–63. <https://doi.org/10.1099/jmm.0.46124-0>.
- (6) Llc, S. C. TRANSLATIONAL RESEARCH SOLUTIONS IMPROVING REPRODUCIBILITY : <https://doi.org/10.1371/journal.pone.0029828>.
- (7) Khatoon, N.; Mazumder, J. A.; Sardar, M. Journal of Nanosciences : Current Biotechnological Applications of Green Synthesized Silver Nanoparticles. **2017**, 2 (1), 1–8. <https://doi.org/10.4172/2572-0813.1000107>.
- (8) Satori, C. P.; Kostal, V.; Arriaga, E. A. Review on Recent Advances in the Analysis of Isolated Organelles. *Anal. Chim. Acta* **2012**, 753, 8–18.
<https://doi.org/10.1016/j.aca.2012.09.041>.
- (9) Cushing, B. L.; Kolesnichenko, V. L.; Connor, C. J. O. Recent Advances in the Liquid-Phase Syntheses of Inorganic Nanoparticles. **2004**, 1385 (504).
<https://doi.org/10.1021/cr030027b>.
- (10) Burneo, S. Santiago Burneo *. **1997**.
- (11) Ahmed, S.; Ahmad, M.; Swami, B. L.; Ikram, S. REVIEW A Review on Plants Extract Mediated Synthesis of Silver Nanoparticles for Antimicrobial Applications : A Green Expertise. *J. Adv. Res.* **2016**, 7 (1), 17–28. <https://doi.org/10.1016/j.jare.2015.02.007>.
- (12) Ledezma, E. Ajoene , El Principal Compuesto Activo Derivado Del Ajo (Allium Sativum), Un Nuevo Agente Antifúngico. *Rev. Iberoam. Micol.* **2006**, 23 (2), 75–80.
[https://doi.org/10.1016/S1130-1406\(06\)70017-1](https://doi.org/10.1016/S1130-1406(06)70017-1).
- (13) Cordova, M. Instituto Politécnico Nacional. **2010**.
- (14) Aizaga Zurita Sofia Jackeline. *EFEECTO ANTIFÚNGICO DEL ACEITE ESENCIAL DE CANELA*; Quito-Ecuador, 2017.
- (15) Carretero, M.; Accame, C. Actividad Terapéutica de La Corteza de Canela. **2010**.
- (16) Junior, W. L. . *ORGANIC CHEMISTRY*, Eighth.; Whitman College, Ed.; Pearson: Boston.

- (17) Manahan, S. E. *GREEN CHEMISTRY AND THE TEN COMMANDMENTS OF SUSTAINABILITY*, Second.; ChemChar Research, Inc: U.S.A, 2005.
- (18) Power, A.; Betts, T.; Cassidy, J. The Bench Synthesis of Silver Nanostructures of Variable Size and an Introductory Analysis of Their Optical Properties. **2013**.
<https://doi.org/10.21427/D75C9Z>.
- (19) Cardeño Calle, L.; Londoño, M. E. Síntesis Verde de Nanopartículas de Plata Mediante El Uso Del Ajo (*Allium Sativum*). *Rev. Soluciones Postgrado EIA* **2014**, *12*, 129–140.
<https://doi.org/http://dx.doi.org/10.14508/sdp.2014.6.12.129-140>.
- (20) Vijaya, N.; Selvasekarapandian, S.; Sornalatha, M.; Sujithra, K. S.; Monisha, S. Proton-Conducting Biopolymer Electrolytes Based on Pectin Doped with NH₄X (X=Cl, Br). *Ionics (Kiel)*. **2017**, *23* (10), 2799–2808. <https://doi.org/10.1007/s11581-016-1852-5>.
- (21) Nithya, S.; Selvasekarapandian, S.; Karthikeyan, S.; Pandi, D. V. Effect of Propylene Carbonate on the Ionic Conductivity of Polyacrylonitrile-Based Solid Polymer Electrolytes. **2015**, *41743*, 1–3. <https://doi.org/10.1002/app.41743>.
- (22) Eustis, S.; El-sayed, M. A.; Kasha, M. Why Gold Nanoparticles Are More Precious than Pretty Gold : Noble Metal Surface Plasmon Resonance and Its Enhancement of the Radiative and Nonradiative Properties of Nanocrystals of Different Shapes. **2006**, 209–217. <https://doi.org/10.1039/b514191e>.
- (23) Anker, J. N.; Hall, W. P.; Lyandres, O.; Shah, N. C.; Zhao, J.; Duynes, R. P. Van. Biosensing with Plasmonic Nanosensors. **2008**, No. July.
<https://doi.org/10.1038/nmat2162>.
- (24) Vincenzo, A.; Roberto, P.; Marco, F.; Onofrio, M. M.; Maria Antonia, I. Surface Plasmon Resonance in Gold Nanoparticles: A Review. *J. Phys. Condens. Matter* **2017**, *29* (20), 203002.
- (25) Egerton, R. F. Physical Principles of Electron Microscopy: An Introduction to TEM, SEM, and AEM, Second Edition. *Phys. Princ. Electron Microsc. An Introd. to TEM, SEM, AEM, Second Ed.* **2016**, 1–196. <https://doi.org/10.1007/978-3-319-39877-8>.
- (26) Inkson, B. J. *Scanning Electron Microscopy (SEM) and Transmission Electron Microscopy (TEM) for Materials Characterization*; Elsevier Ltd, 2016.
<https://doi.org/10.1016/B978-0-08-100040-3.00002-X>.
- (27) Xu, R. Progress in Nanoparticles Characterization : Sizing and Zeta Potential Measurement. **2008**, *6*, 112–115. <https://doi.org/10.1016/j.partic.2007.12.002>.
- (28) Gómez, G. L. Nanopartículas de Plata : Tecnología Para Su Obtención , Caracterización Y Actividad Biológica. **2013**.
- (29) Lara, H. H.; Ayala-Núñez, N. V.; del Turrent, L. C. I.; Padilla, C. R. Bactericidal Effect of Silver Nanoparticles against Multidrug-Resistant Bacteria. *World J. Microbiol. Biotechnol.* **2010**, *26* (4), 615–621. <https://doi.org/10.1007/s11274-009-0211-3>.

- (30) Scientific, E.; Ireland, P.; Stalberg, E.; Nandedkar, S.; Stalberg, S.; General, T. Technical Section. **1983**, *45* (4), 672–681.
- (31) Ramírez, N.; Regueiro, A.; Arias, O.; Contreras, R. Espectroscopía de Impedancia Electroquímica, Herramienta Eficaz Para El Diagnóstico Rápido Microbiológico. **1989**, *31* (2).
- (32) Values, C. I.; Electrochemistry, P.; Elements, C.; Equivalent, C.; Models, C. Basics of Electrochemical Impedance Spectroscopy. No. 1.
- (33) Flores, J. M.; Romero, R. D.; Llongueras, J. G.; Mexicano, I. NOTAS. 1–33.
- (34) Saha, M.; Bandyopadhyay, P. K. Green Biosynthesis of Silver Nanoparticle Using Garlic , *Allium Sativum* with Reference to Its Antimicrobial Activity Against the Pathogenic Strain of *Bacillus Sp .* and *Pseudomonas Sp .* Infecting Goldfish , *Carassius Auratus*. *Proc. Zool. Soc.* **2017**. <https://doi.org/10.1007/s12595-017-0258-3>.
- (35) Method, I.; Information, B. Gold and Silver Nanoparticles. *North* **2008**, 1–7.
- (36) Gruhlke, M. C. H.; Slusarenko, A. J. The Biology of Reactive Sulfur Species (RSS). *Plant Physiol. Biochem.* **2012**, *59*, 98–107. <https://doi.org/10.1016/j.plaphy.2012.03.016>.
- (37) Pike, E. R. *Introduction to Soft X-Ray Spectroscopy*; 2005; Vol. 28. <https://doi.org/10.1119/1.1935107>.
- (38) Huang, S. T.; Xu, X. N. Synthesis and Characterization of Tunable Rainbow Colored Colloidal Silver Nanoparticles Using Single-Nanoparticle Plasmonic Microscopy and Spectroscopy. **2010**, No. 207890. <https://doi.org/10.1039/c0jm01990a>.
- (39) Millan, F. *MÉTODOS ESPECTROSCÓPICOS UV VISIBLE PARA ANÁLISIS MOLECULAR Y ELEMENTAL*; INSTITUTO UNIVERSITARIO POLITÉCNICO SANTIAGO MARÍNÑO, Ed.; 2016. <https://doi.org/10.13140/RG.2.2.16927.15528>.
- (40) Shakeri-Zadeh, A.; Mansoori, Ga. Cancer Nanotechnology Treatment through Folate Conjugated Gold Nanoparticles (*). *Proc. WCC* **2010**, *2010*, 1–5.
- (41) Saade, J.; Araújo, C. B. De. Synthesis of Silver Nanoprisms : A Photochemical Approach Using Light Emission Diodes. *Mater. Chem. Phys.* **2014**, *148* (3), 1184–1193. <https://doi.org/10.1016/j.matchemphys.2014.09.045>.
- (42) Frank, A. J.; Cathcart, N.; Maly, K. E.; Kitaev, V. Synthesis of Silver Nanoprisms with Variable Size and Investigation of Their Optical Properties: A First-Year Undergraduate Experiment Exploring Plasmonic Nanoparticles. *J. Chem. Educ.* **2010**, *87* (10), 1098–1101. <https://doi.org/10.1021/ed100166g>.
- (43) Mahendia, S.; Tomar, A. K.; Kumar, S. Electrical Conductivity and Dielectric Spectroscopic Studies of PVA-Ag Nanocomposite Films. *J. Alloys Compd.* **2010**, *508* (2), 406–411. <https://doi.org/10.1016/j.jallcom.2010.08.075>.
- (44) Sánchez, M.; Álvarez, J. Nanopartículas de Plata: Preparación, Caracterización Y Propiedades Con Aplicación En Inocuidad de Los Alimentos. *Lab. Complement. Quim. .*

